SYNTHESIS AND CHARACTERIZATION OF RUTHENIUM(0) NANOPARTICLES AS CATALYST IN THE HYDROLYSIS OF SODIUM BOROHYDRIDE

A THESIS SUBMITTED TO
THE GRADUATE SCHOOL OF NATURAL AND APPLIED SCIENCES
OF
MIDDLE EAST TECHNICAL UNIVERSITY

BY

MEHMET ZAHMAKIRAN

IN PARTIAL FULFILLMENT OF THE REQUIREMENTS
FOR
THE DEGREE OF MASTER OF SCIENCE
IN
CHEMISTRY

APRIL 2005

Approval of the Graduate School of Natural and Applied Sciences

_____

Prof.Dr. Canan Özgen

Director

I certify that this thesis satisfies all the requirements as a thesis for the degree of Master of Science.

_____

Prof. Dr. Hüseyin İşçi

Head of the department

This is to certify that we have read this thesis and that in our opinion it is fully adequate, in scope and quality, as a thesis for the degree of Master of Science.

_____

Prof. Dr. Saim Özkâr

Supervisor

Examining Committee Members

Prof. Dr. Hüseyin İşçi	(METU, CHEM)	_____
Prof. Dr. Saim Özkâr	(METU, CHEM)	_____
Prof. Dr. H. Ceyhan Kayran	(METU, CHEM)	_____
Prof. Dr. Işık Önal	(METU, CHE)	_____
Doc. Dr. Gülsün Gökağaç	(METU, CHEM)	_____

I hereby declare that all information in this document has been obtained and presented in accordance with academic rules and ethical conduct. I also declare that, as required by these rules and conduct, I have fully cited and referenced all material and results that are not original to this work.

Name, Last name :

Signature :

ABSTRACT

SYNTHESIS AND CHARACTERIZATION OF RUTHENIUM(0) NANOPARTICLES AS CATALYST IN THE HYDROLYSIS OF SODIUM BOROHYDRIDE

Zahmakıran, Mehmet
M.S., Department of Chemistry
Supervisor: Prof. Dr. Saim Özkâr

April 2005, 78 pages

Sodium borohydride is stable in alkaline solution, however, it hydrolyses and generates hydrogen gas in the presence of suitable catalyst. By this way hydrogen can be generated safely for the fuel cells. All of the catalyst having been used in the hydrolysis of sodium borohydride, with one exception, are heterogeneous. The limited surface area of the heterogeneous and therefore, have limited activity because of the surface area. Thus, the use of metal nanoclusters as catalyst with large surface area is expected to provide a potential route to increase the catalytic activity.

In this dissertation we report for the first time the use of ruthenium(0) nanoparticles as catalyst in the hydrolysis of sodium borohydride. The water dispersible ruthenium(0) nanoparticles were prepared by the reduction of $RuCl_3.xH_2O$ with sodium borohydride and were stabilized by three different ligands dodecanethiol, ethylenediamine and acetate. Among these three colloidal materials the acetate stabilized ruthenium(0) nanoparticles were found to have the highest catalytic activity in catalyzing the hydrolysis of sodium borohydride. The acetate stabilized ruthenium(0) nanoparticles were characterized by tranmission electron microscopy (TEM), X-ray photoelectron spectroscopy and FT-IR spectroscopy. The particle size of the acetate stabilized ruthenium(0) nanoparticles was determined to be 2.62±1.18 nm from the TEM analysis. The kinetic of the ruthenium(0) nanoparticles catalyzed hydrolysis of sodium borohydride was studied depending on the catalyst concentration, substrate concentration and temperature. The activation parameters of this reaction were also determined from the evaluation of the kinetic data. This catalyst provides the lowest activation energy ever found for the hydrolysis of sodium borohydride.

Keywords: Sodium borohydride; Ruthenium(0) nanoparticles; Transmission electron microscopy (TEM); X-Ray photoelectron spectroscopy (XPS); Homogeneous catalyst

ÖZ

SODYUM BORHİDRÜRÜN HİDROLİZİNİ KATALİZLEYEN RUTENYUM(0) NANOKÜMELERİNİN SENTEZLENMESİ VE TANIMLANMASI

Zahmakıran, Mehmet
Yüksek Lisans, Kimya Bölümü
Tez Yöneticisi: Prof. Dr. Saim Özkâr

Nisan 2005, 78 sayfa

Sodyum borhidrür alkali çözeltilerde kararlı olmasına karşın suda uygun bir katalizör eşliğinde hidrolizi sonucu hidrojen gazı açığa çıkarır. Bu yolla yakıt pilleri için gerekli olan hidrojen gazı güvenli şekilde sağlanabilir. Bugüne kadar sodyum orhidrürün hidrolizinde kullanılan katalizörlerin biri dışında hepsi heterojendir, bu yüzden bu katalizörlerin katalitik etkinlikleri sınırlı yüzey alanlarından dolayı sınırlıdır. Bu bağlamda metal nanokümelerin katalizör olarak kullanımı, sahip oldukları geniş yüzey alanlarından dolayı, katalitik etkinliği arttıran potansiyel bir yöntem olarak beklenilmektedir.

Bu tezde ilk kez rutenyum nanokümelerinin sodyum borhidrürün hidrolizinde katalizör olarak kullanımını sunuyoruz. Rutenyumun suda çözünen nanokümeleri, sulu çözeltide $RuCl_3.xH_2O$ tuzunun indirgenmesi ve daha sonra üç farklı ligantla dodekantiyol, etilendiamin ve asetat ile kararlı hale getirilmeleriyle hazırlandı. Hazırlanan farklı kolloit haldeki materyalle arasında asetat ile kararlı hale getirilen rutenyum(0) nanokümeleri sodyum borhidrürün hidrolizinde en yüksek katalitik etkinliği gösterdi. Asetat ile kararlı hale getirilen rutenyum(0) nanokümelerinin tanecik büyüklüğü 2.62±1.18 nm olarak hesaplandı. Asetat ile kararlı hale getirilen rutenyum(0) nanokümeleri tarafından katalizlenen sodyum borhidrürün hidroliz tepkimesinin kinetiğide katalizör derişimine, sodyum borhidrür derişimine, kararlaştırıcı asetatın derişimine ve sıcaklığa bağlı olarak çalışıldı. Tepkime için geçerli olan aktivasyon parametreleri kinetik sonuçlarının ışığında hesaplandı. Bu katalizör şimdiye kadar bulunan en düşük aktivasyon enerjisini sağladı.

Anahtar kelimeler: Sodyum borhidrürün hidrolizi; Rutenyum(0) nanokümeleri; Transmisyon elektron mikroskopisi (TEM); X-ışınları fotoelektron spektroskopisi (XPS); Homojen katalizör.

To My Family

ACKNOWLEDGEMENTS

I would like to express my sincere gratitude to Prof. Dr. Saim Özkâr for his great support, supervision and understanding throughout in this study.

I would like to thank Özgür Başer, Murat Rakap, Fatma Alper, Ercan Bayram, Pelin Erdinç, Sanem Koçak, Cüneyt Kavaklı, Ceyhun Akyol, , Dilek Ayşe Boğa, and Ezgi Keçeli for their caring, never ending helps and their encouragement during my study.

I also give my thanks to the members of the Chemistry Department of Middle East Technical University for providing facilities used in this study.

The last but not least, I would like to extend my gratitude to my father, Turhan, my mother, Kadriye, and my sister, Betül, for helping me with every problem I encountered during the whole study.

TABLE OF CONTENTS

LIST OF TABLES

TABLE

LIST OF FIGURES

FIGURE

CHAPTER 1

INTRODUCTION

1.1. Energy Related Global Problems

Soon after the invention of the steam engine in the 1860's, when the industrial revolution started to replace human and beast toil with nature's energy sources, a bright future seemed to be certain for humankind. More and more of nature's energy, initially in the form of wood and coal, and later as oil and natural gas, were being harnessed for the benefit of humans. This resulted in the mass production of goods, with a corresponding reduction in prices and rising living standards. Fossil fuels which fed this amazing economic growth were the medicine to cure deprivation. But it was an untested medicine at that. As planet Earth consumed more and more fossil fuels, two important predicaments started to emerge: (1) the fossil fuels would be depleted in a foreseeable future, and (2) the fossil fuels and their combustion products were causing global environmental problems. The demand for energy continues to rise because of the continuing increase in world population, and the growing demand by the developing countries in order to improve their living standards. At the present time, a large portion (about 70%) of the world energy demand is met by the fossil fuels because of their availability and convenient use. However, it is expected that the world's fossil fuels production will soon peak and thereafter begin to decrease. It is estimated that,[1] the fluid fossil fuel (petroleum and natural gas) production world wide will continue to rise for the next 15 years, and

then will start to decrease. In the meantime, as a result of the growing world population and the desire of the people to better their living standarts, the world energy consumption is projected to increase 70% up to the year 2030 and the average increase is 1.8% per year and to be doubled by the year 2050.[2] There will be a growing gap, starting within the next ten years between the demand and production of fuels.

The second predicament involving the fossil fuels is the environmental damage being caused by the fossil fuels and their combustion products. Technologies for fossil fuel extraction, transportation, processing and particularly their end use, combustion have harmful impact on the environment, which cause direct and indirect negative effects on the economy. Conventional petroleum based fuels like gasoline or diesel, as well as, natural gas and coal, all contain carbon. When these fuels are burned, their carbon recombines with oxygen from the air to form carbon dioxide (CO_2), the primary greenhouse gas that causes global warming. Furthermore, combustion of fossil fuels produces other toxic emissions.

Carbon monoxide (a poison), oxides of nitrogen and sulfur (NOx, SOx), volatile organic chemicals and fine particulates are all components of air pollution attributable to the refining and combustion of fossil fuels. When released into the atmosphere many of these compounds cause acid rain or react with sunlight to create ground-level smog. Vast ecosystem damage, increase lung disease and cancer are the ultimate price we pay for consuming these fossil fuels.

1.2. Hydrogen Economy

Because of the aforementioned problems, it is widely studied to find possible energy sources to replace the fossil fuels. There are quite number of primary energy sources available such as thermonuclear energy, nuclear breeders, tides, waves, solar energy, wind energy, hydropower, geothermal energy and ocean streams. Among these different energy sources, hydrogen boasts many important advantages as an energy carrier: it is abundant, secure, clean to be used, renewable, and widely available from diverse sources. Using hydrogen as an energy carrier in energy efficient fuel cells, in which the energy obtained upon a reaction of hydrogen and oxygen is directly converted into electrical energy, [3] can fundamentally change our relationship with the natural environment.

Hydrogen production, storage and distribution methods are commercially available today, but dramatic improvements, particularly of existing technologies, are needed if hydrogen is to become a major energy carrier in the future. As a result of the above discussion, the importance of hydrogen economy is getting increase. The hydrogen based energy economy needs three basic research stages;

(i) Development of diversity of methods for hydrogen production from renewable energy sources. Despite its abundance in nature, hydrogen is not a primary energy source and must be produced from a primary energy source such as fossil hydrocarbons or coal, nuclear fusion or fission, hydroelectric, or renewable energy sources. Depending on the source, its production may or may not involve CO_2 emissions.

(ii) Lowering the cost of fuel cells and improving their usage on-board systems. Hydrogen is an ideal anodic fuel for Proton Exchange Membrane,

PEM, fuel cells that convert chemical energy of hydrogen into electrical energy, heat and water in a clean, quiet manner with little or no enviromentally harmful by-products. Until large PEM fuel cells become commercially available, internal combustion engines fueled with H_2 could represent a backup option for upcoming zero emission vehicle, ZEV, mandates for transportation applications. In internal combustion applications, H_2 can be considered more thermally efficient than gasoline primarily because it burns better in excess air, and permits use of higher compression ratios. H_2 can burn in lean as well as rich air mixtures; it can improve fuel use efficiencies in start-stop type of city driving.

(iii) Finding viable methods for hydrogen storage. Advanced hydrogen storage concepts include metal hydrides, complex hydrides, alanates, carbon adsorption and nanostructured materials, carbon nano-tube encapsulation. Key criteria for succesful use of hydrogen in the transportation market is the energy density of the storage system, as compared to other fuels.

1.3. Sodium Borohydride As A Hydrogen Storage Material

Recently, as a new fueling concept, it can be suggested that the chemical hydrides ($NaBH_4$, KBH_4, LiH, NaH, etc.) act as new fuel source supplying hydrogen at normal temperature.[4] Chemical hydrides are very reactive toward hydrolysis in water, which results in releasing a large amount of hydrogen gas. Among these chemical hydrides, sodium borohydride ($NaBH_4$) is in the group of highest energy content, both weight basis and volume basis[5] shown in Figure 1.1. Also it is a safe and practical means of producing hydrogen, but it's sensitive to moisture in air.

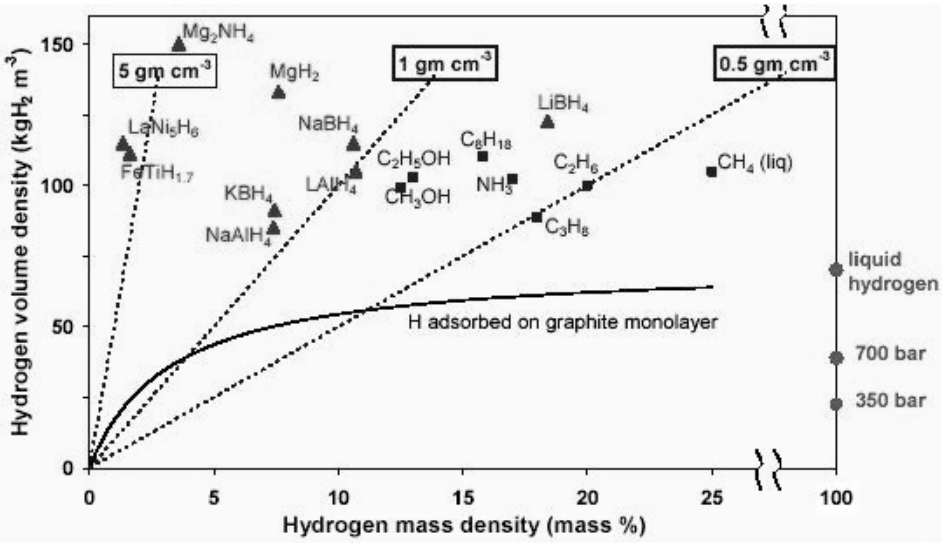

Figure 1.1. Volumetric hydrogen density versus gravimetric hydrogen density of various hydrogen containing compounds (taken from the literature[4]).

Hydrolysis of $NaBH_4$, produces hydrogen gas and water-soluble sodium metaborate, $NaBO_2$, in the presence of a suitable catalyst.[6] By this way, hydrogen can be generated safely for the fuel cells.

$$NaBH_4 + 2H_2O \xrightarrow{\text{catalyst}} NaBO_2 + 4H_2 \quad \textbf{(1)}$$

Generating H_2 catalytically from $NaBH_4$ solutions has many advantages: $NaBH_4$ solutions are nonflammable, reaction products are environmentally benign, rate of H_2 generation can be easily controlled, the reaction product $NaBO_2$ can be recycled, H_2 can be generated even at low temperatures. Such a hydrolysis of sodium borohydride can be accelerated by catalysts,[7] by acid,[8] or under elevated temperature.[9]

This reaction occurs to some extent even without a catalyst if the solution pH < 9. However to increase the shelf life of $NaBH_4$ solutions and to prevent H_2 gas from being slowly produced upon standing, $NaBH_4$

solutions are typically maintained as a strongly alkaline solution by adding NaOH. The key feature of using a catalyzed reaction to produce H_2 is that H_2 generation in alkaline (pH > 7) $NaBH_4$ solutions occur only when these solutions contact with selected heterogeneous catalysts. Without catalyst present, strongly alkaline $NaBH_4$ solutions do not produce appreciable H_2. This reaction is extremely efficient on a weight basis, since out of the 4 moles of H_2 that is produced, half comes from $NaBH_4$, and the other half from H_2O. Reaction is exothermic, so no energy input is needed to generate H_2.

To generate H_2 at the point of use, this easily and air-storable solution containing dissolved $NaBH_4$ is simply allowed to contact with a catalyst. One clear advantage of this method is that rapid H_2 generation can be achieved at ambient temperatures (and even down to 0 $^{\circ}$C) without mechanical compression, addition of water, acid or heat. In addition, since stabilized $NaBH_4$ solutions without catalyst produce very little H_2, and H_2 is only generated as needed, safety concerns about onboard storage of free H_2 are reduced.

In the presence of water

$$BH_4^- + 2H_2O \longrightarrow BO_2^- + 4H_2 \qquad \textbf{(2)}$$

In the presence of acids

$$BH_4^- + H^+ + 3H_2O \longrightarrow H_3BO_3 + 4H_2 \qquad \textbf{(3)}$$

The only other product of reaction, sodium metaborate (in solutions with pH > 11, the predominant solution product is sodium tetrahydoxyborate $NaB(OH)_4$, is water soluble and environmentally innocuous. Since the hydrolysis of sodium borohydride is a completely inorganic reaction and does not contain sulfur, it produces virtually no fuel poisons such as sulfur compounds, carbon monoxide, soot, or aromatics.

Therefore this reaction is considerably safer, more efficient, and easily controllable than producing H_2 by other chemical methods.[10] The heat generated by the reaction 75 kJ per mole of H_2 formed is considerably less than typical > 125 kJ/mole H_2, produced by reacting other chemical hydrides with water.[11] This promises a safer and more controllable reaction.

All of the catalysts used in hydrolysis of sodium borohydride so far are bulk metals and they act as heterogeneous catalysts.[12] The limited surface area of the heterogeneous catalysts leads to a lower catalytic activity, as the activity of catalyst is directly related to its surface area. Thus, the use of metal nanoclusters with large surface area provides a potential route to increase the surface area and, thus, the catalytic activity.[13]

Transition metal nanoclusters hold the potential to be active and selective catalysts since a large percentage of atoms are on the surface. On the other hand, nanoclusters provide the possibility of controlling both the particle size and surface coverage (i.e., availability of the surface atom) by stabilizing material in a quantitative and modifiable way than previously possible in the heterogeneous catalysts. This dissertation work aims the use of the transition metal nanoclusters in catalyzing the hydrolysis of sodium borohydride to generate hydrogen gas at low temperature. In addition to its' industrial importance, this dissertation work also provides a fundamental understanding of the formation and stabilization of transition metal nanoclusters in aqueous media. This understanding is vital in the preparation of transition metal nanoclusters which are stable enough as a dispersed phase, but still catalytically active for example, in the hydrolysis of sodium borohydride. It is novel as reporting for the first time the results of our study on the hydrogen generation from the catalytic hydrolysis of sodium borohydride using water-dispersible ruthenium(0) nanoclusters as catalyst.

CHAPTER 2

INTRODUCTORY CONCEPTS OF CATALYSIS

2.1. Introduction And Definitions

Nitrogen and hydrogen flows through a tube at high temperature and pressure, but they do not react to give ammonia, although the chemical equilibrium is favorable. When particles of iron are placed in the tube, however the gases coming in contact with them are converted rapidly into ammonia. Millions of kilograms of this chemical are synthesized every year in such tubular reactors at a cost of few cents per kilogram. Ammonia is a raw material for nitrate fertilizers needed to feed the world's population. Fertilizers are assimilated by the cells of plants in complex sequences of biological reactions. Further metabolic reactions take place as animals consume the plants, reconstructing their contents to provide energy and molecular building blocks for growth. All these biological reactions are catalyzed by naturally occurring macromolecules called enzymes.

What is an enzyme, and what does it have in common with the iron in the ammonia synthesis reactor? Each is a catalyst- a substance that alters the rate of reaction without appearing in any of the products of that reaction; it may speed up or speed down a reaction. For a reversible reaction, a catalyst alters the rate at which equilibrium is attained; it does not alter the position of equilibrium.

The term catalyst is often used to encompass both the catalyst precursor and the catalytically active species. A catalyst precursor is the substance added to the reaction, but it may undergo loss of a ligand such as CO or PPh_3 before it is available as the catalytically active species.

Although one tends to associate a positive catalyst with increasing the rate of reaction, a negative catalyst slows down a reaction. Some reactions are internally catalyzed (autocatalysis) once the reaction is under way, e.g. in the reaction of $[C_2O_4]^{2-}$ with $[MnO_4]^-$, the Mn^{2+} ions formed catalyze the forward reaction, so in an autocatalytic reaction, one of the products is able to catalyze the reaction. Catalysts fall into two categories, homogeneous and heterogeneous depending on their relationship to the phase of the reaction in which they are involved. A homogeneous catalyst is in the same phase of the reaction that it is catalyzing; a heterogeneous catalyst is in a different phase from the components of the reaction for which it is acting.

2.2. Free Energy Profile

A catalyst operates by allowing a reaction to follow a different pathway from that of non-catalyzed reaction. If the activation barrier is lowered, then the reaction proceeds more rapidly. Figure 2.1 illustrates this for a reaction that follows a single step when it is non-catalyzed, but a four steps path when a catalyst is added. Each step in the catalyzed route has a characteristic free energy of activation, $\Delta G^{\#}$, but the step that matters with respect to the rate of reaction is that with higher barrier; for the catalyzed pathway. A crucial aspect of the catalyzed pathway is that it must not pass through an energy minimum lower than the energy of products- such a minimum would be an 'energy sink' and would lead to the pathway yielding different products from those desired.

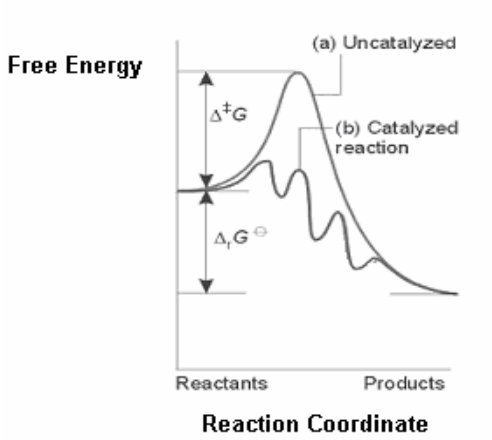

Figure 2.1. A schematic representation of the reaction profile of a reaction without and with catalyst.

2.3. Catalytic Cycles

A catalyzed reaction pathway is usually represented by a catalytic cycle. A catalytic cycle consists of a series of stoichiometric reactions (often reversible) that form a closed loop; the catalyst must be regenerated so that it can participate in the cycle of reactions more than once. For a catalytic cycle to be efficient, the intermediates must be short-lived. The downside of this for understanding mechanism is that short lifetimes make studying a cycle difficult. Experimental probes are used to investigate the kinetics of a catalytic process, isolate or trap the intermediates, attempt to monitor intermediates in the cycle. As an example Figure 2.2 shows the catalytic cycle of Wacker process, is primarily used to produce acetaldehyde from ethene, and oxygen.

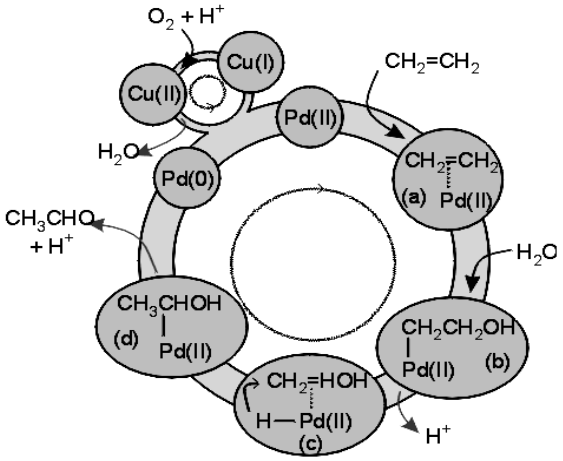

Figure 2.2. Catalytic cycle for the Wacker process.(Adapted from the literature[14])

2.4. Properties Of Catalysts

A reaction is not usually catalyzed by a unique species and a number of criteria must be considered when choosing the most effective catalyst, especially for a commercial process. Apart from the changes in reaction conditions that the use of catalyst may bring about (e.g., pressure, temperature), other factors that must be considered are: the concentration of catalyst required, the catalytic turnover, the selectivity of the catalyst to the desired product, how often the catalysts need renewing.

2.4.1. Turnover Frequency (TOF), And Turnover Number (TON)

The catalytic turnover number (TON) is the number of moles of product per mole of catalyst; this number indicates the number of catalytic cycles for a given process, e.g. after 2 hours the TON was 2400. The catalytic turnover frequency (TOF) is the catalytic turnover per unit time:

the number of moles of product per mole of catalyst per unit time, e.g. the TOF was 20 min^{-1}.

If we consider the conversion of A to B catalyzed by Q and with a rate v the catalytic turnover number and turnover frequencies can be given as follows.

$$A \xrightarrow{Q} B \quad v = \frac{d[B]}{dt} \qquad \textbf{(1)}$$

$$TON = \frac{[B]}{[Q]} = \frac{\text{moles of product}}{\text{moles of catalyst}} \quad \textbf{(2)}$$

$$TOF = \frac{v}{[Q]} = \frac{\text{moles of product}}{\text{moles of catalyst} \times \text{time}} \quad \textbf{(3)}$$

Defining the catalytic turnover number and frequency is not without problems. For example, if there is more than one product, one should distinguish between values of the total TON and TOF for all the catalytic products, and specific values for individual products. The term catalytic turnover number is usually used for batch processes, where as catalytic turnover frequency is usually applied to continuous process.

2.4.2. Selectivity

A selective catalyst yields a high proportion of the desired product with minimum amounts of side products. In industry, there is considerable economic incentive to develop selective catalysts. For example, when metallic silver is used to catalyze the oxidation of ethene with oxygen to

produce ethylene oxide, the reaction is accompanied by the more thermodynamically favored but undesirable formation of CO_2 and H_2O. This lack of selectivity increases the consumption of ethane, so chemists are constantly trying to devise a more selective catalyst for this reaction. Selectivity can be ignored in only a very few simple inorganic reactions where there is essentially only one thermodynamically favorable product, as in the formation of NH_3 from H_2 and N_2. Figure 2.3 shows the selectivity of each catalyst in the reaction of ethene with oxygen, it indicates the choice of catalyst can have a significant effect on the yield of the desired product.

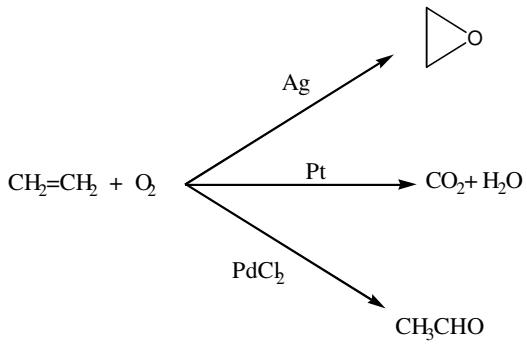

Figure 2.3. The reaction of ethene with oxygen in the presence of different catalysts yields different major products.

2.4.3. Lifetime

A small amount of catalyst must survive through a large number of cycles if it is to be economically viable. However, a catalyst may be destroyed by side reactions to the main catalytic cycle or by the presence of small amounts of impurities in the starting materials. Therefore, a catalyst is also chosen on the basis of its' stability: the greater stability, the lower

the rate at which the catalyst loses its' activity or selectivity or both. A deactivated catalyst may be treated to bring back its' activity; its' regenerability in such a treatment is a measure of how well its' activity can be brought back.

2.5. Importance Of Size Reduction Of Catalysts

Surface chemistry is of vital importance in numerous processes, including corrosion, adsorption, oxidation-reduction and catalysis. Particles in the 1-10 nm range open a new vista in surface chemistry because surface-reactant interactions can become stoichometric, this is due to two reasons. First, the huge surface areas of the nanostructured material dictate that many of the atoms are on the surface, thus allowing good 'atom economy' in surface-gas, surface-liquid, or even surface-solid reactions. Figure 2.4 illustrates the calculated numbers of iron atoms on the surface of spherical iron nanoclusters and the iron atoms in the bulk.

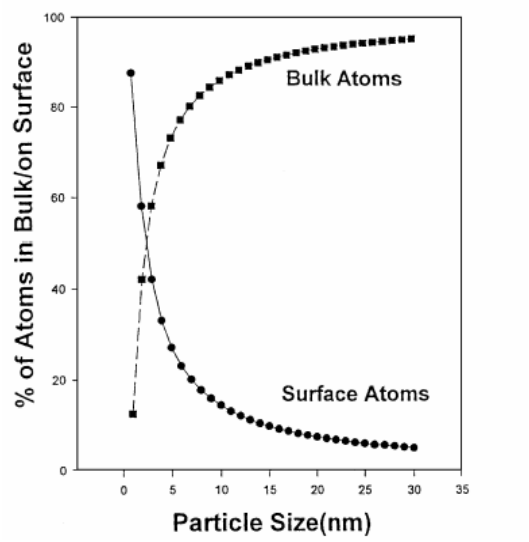

Figure 2.4. Calculated surface to bulk atom ratios for spherical iron nanoparticles (Adapted from the reference[15]).

Note that quite small sizes are necessary; indeed, a 3 nm particle has 50% of the atoms on the surface, while a 20 nm particle has fewer than 10%. This demonstrates that it is necessary to get small particles in order to benefit from the atom economy desired. A second aspect of surface chemistry that nanoclusters' feature is enhanced intrinsic chemical reactivity as size gets smaller. The increasing proportion of surface atoms with decreasing particle size, compared with bulk metals, makes small metal particles become highly reactive catalysts, as surface atoms are the active centers for catalytic elementary processes. Among the surface atoms, those sitting on the edges and corners are more active than those in planes. The percentage of edge and corner atoms also increases with decreasing size and this is why very small particles are preferred as catalysts (Figure 2.5 shows this effect clearly).

Full-shell Clusters		Total Number of Atoms	Surface Atoms (%)
1 Shell		13	92
2 Shells		55	76
3 Shells		147	63
4 Shells		309	52
5 Shells		561	45
7 Shells		1415	35

Figure 2.5. The relation between the total number of atoms in full shell clusters and the percentage of surface atoms.

Among the chemical properties of transition metal nanoclusters discussed above, catalysis is of great interest because of their high surface to volume ratio and a unique combination of reactivity, stability, and selectivity. Transition metal nanoclusters have been shown to be effective catalysts for many chemical transformations. Examples include; spanning hydrogenations,[16] enantioselective hydrogenations,[17] hydrosilylations,[18] hydropyrolysis and hydrogenolysis, oxidation of CO and $CO/H_{2,}$[19] oxidative acetoxylation,[20] McMurry,[21] Suzuki[22] and Heck-Type[23] couplings, and, [3+2] cycloaddition reactions.[24] The majority of these reactions have been performed by nanoclusters deposited on a heterogeneous support.

CHAPTER 3

TRANSITION METAL NANOCLUSTERS

3.1. Colloidal Transition Metal Nanoclusters

Interest in colloidal metal particles exemplified by aqueous gold solutions dates back to time of Michael Faraday in 1831, he recognized that the different colors in gold solutions could be indicative of different sizes or states of aggregation of the particles. Nanoparticles near monodispersed particles that are generally less than 10 nm in diameter[25] have generated intense interest over the past decade. One reason for this is the belief that nanoclusters will have unique properties, derived in part from the fact that these particles and their properties lie somewhere between those of bulk and single particle species[26]. Nanoparticles have many fascinating potential uses, including quantum dots[27] and quantum computers[28] and devices,[29] chemical sensors,[30] light-emitting diodes,[31] photochemical pattern applications such as flat-panel displays.[32] Nanoparticles also have significant potential as new types of highly active and selective catalysts.[33]

Transition metal nanoclusters are expected to have unique physical and chemical properties due to two factors. One is the quantum size effect.[34] The illustration of the electronic states from a metal particle with bulk properties to a simple atom is given in Figure 3.1.

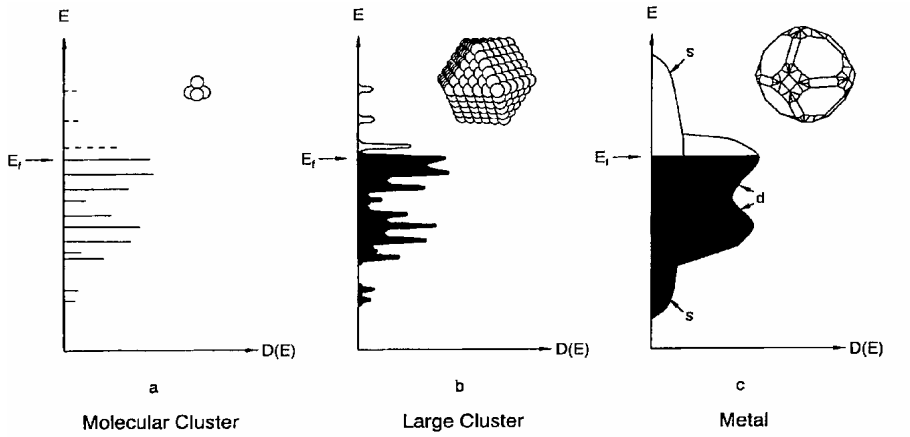

Figure 3.1. Illustration of the electronic states of (a) isolated atoms with well separated bonding and antibonding molecular orbitals (b) a nanocluster with a small band gap, (c) a metal particle with bulk properties and its typical band structure, (Adapted from the literature[34]).

When a metal particle with bulk properties is reduced to the nanometer size scale, the density of states in the valence and the conduction band decreases to such an extent that the quasi-continuous density of states is replaced by a discrete energy level structure and the electronic properties change dramatically. The other factor is that nanoclusters have a high surface to volume ratio. Figure 3.2 shows an example that when a cube of metal divided into smaller and smaller cubes, more and more atoms are located on the surface of particles.

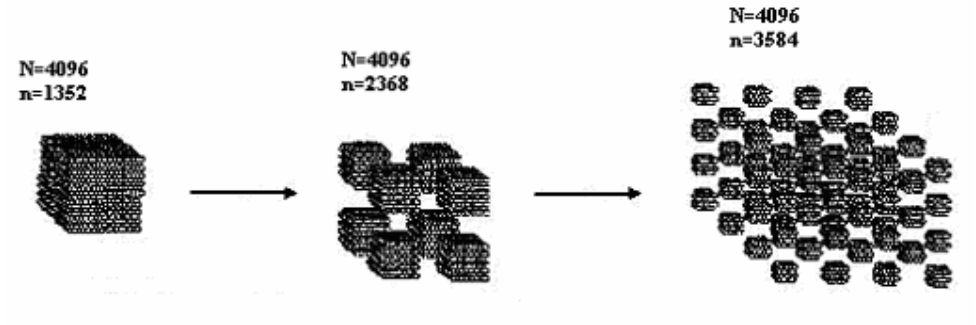

Figure 3.2. The effect of particle size on the ratio of the number of surface atoms to the total number of atoms. N= the total number atoms; n= the number of surface atoms.

To investigate the physical and chemical properties of transition metal nanoparticles, the preparation of these metal particles in monodispersed form and therefore a great degree of control over size, structure, and surface composition is essentially required.

3.2. Stabilization Of Collodial Metal Nanoclusters

One of the main characteristics of colloidal metal nanoclusters is their small size. Unfortunately, these metallic nanoclusters are unstable with respect to agglomeration to the bulk. In most cases, this aggregation leads to the loss of the properties associated with the colloidal state of these metallic particles. For example, during catalysis the coagulation of colloidal particles used as catalyst leads to a significant loss of activity. The stabilization of metallic nanoparticles and thus the means to preserve their finely dispersed state is a crucial aspect to consider during their synthesis. Several general discussions on the stability of metal nanoparticles have already been reported[35]. At short interparticle distances the van der Waals forces will attract two metallic particles to each other. These forces vary

inversely as the sixth power of the distance between their surfaces. In the absence of repulsive forces opposed to the van der Waals forces, the colloidal metal particles will aggregate. In this situation the major source of kinetic stability of colloids is the existence of electrical charge on the surfaces of the particles. On account of this charge, ions of opposite charge tend to cluster nearby, and an ionic atmosphere is formed, just as for ions. Two regions of charge must be distinguished. First, there is a fairly immobile layer of ions that adhere tightly to the surface of the colloidal particle. Second the charged unit attracts an oppositely charged atmosphere of mobile ions. The inner shell of charge and the outer ionic atmosphere is called the electrical double layer. The theory of the stability of colloidal metal particles was developed by B. Derjaguin and L. Landau and independently by E. Verwey and J.T.G. Overbeek, and is known as the DLVO theory.[36] It assumes that there is a balance between the repulsive interaction between the charges of the electrical double layers on neighboring particles and the attractive interactions arising from van der Walls interactions between the molecules in the particles.

Consequently, the use of a stabilizing agent able to induce a repulsive force opposed to the van der Waals forces is necessary to provide stable nanoparticles in solution. The stabilization of metal nanoparticles is usually discussed in terms of four general categories: (i) electrostatic stabilization, (ii) steric stabilization, (iii) electrosteric stabilization, (iv) stabilization by a ligand or solvent.

(i) Electrostatic Stabilization: Ionic compounds such as halides, carboxylates or polyoxoanions, dissolved in (generally aqueous) solution can generate the electrostatic stabilization. The adsorption of these compounds and their related counterions on the metallic surface will generate an electrical double-layer around the particles (Figure 3.3). This results in a Coulombic repulsion between the particles. If the electric

potential associated with the double layer is high enough, then the electrostatic repulsion will prevent particle aggregation.

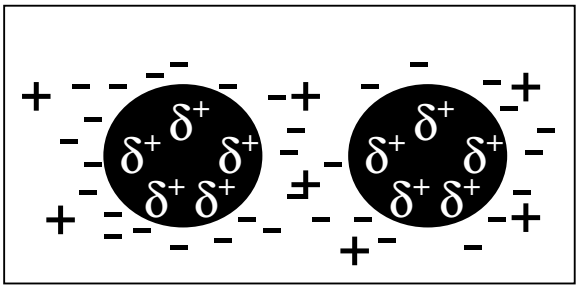

Figure 3.3. Schematic representation of electrostatic stabilization of metal nanoparticles.

(ii) Steric stabilization: It is achieved by surrounding the metal clusters by layers of material that are sterically bulky, such as polymers or oligomers. These large adsorbates provide a steric barrier which prevents close contact of the metal particle center (Figure 3.4).

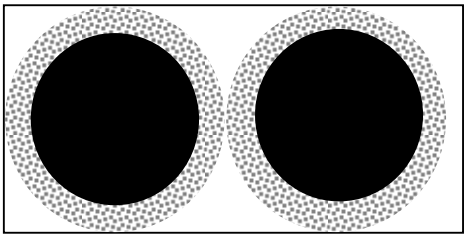

Figure 3.4. Schematic representation of steric stabilization of metal nanoparticles.

(iii) Electrosteric Stabilization: The electrostatic and steric stabilization can be combined to maintain stable metallic nanoparticles in solution. This kind of stabilization is generally provided by means of ionic surfactants. These compounds bear a polar head group able to generate an electrical double layer and a lyophilic side chain able to provide steric repulsion. The electrosteric stabilization can be also obtained by long chain tetraalkylammonium salts of (Bu_4N^+)/ $(P_2W_{15}Nb_3O_{62}^{9-})$.[37]

(iv) Stabilization by a Ligand or Solvent: The term ligand stabilization describes the use of traditional ligands to stabilize transition metal colloids. This stabilization occurs by the coordination of metallic nanoparticles with ligands such as phosphines, thiols, amines or carbon monoxide. It has also reported that nanoparticles can be stabilized only by solvent molecules. Thus Ti[38] and Ru[39] nanoparticles were synthesized in tetrahydrofuran or thioethers without adding steric or electrostatic stabilizers.

3.3. Preparation Of Metal Nanoclusters

Nanostructured metal colloids have been obtained by both “top-down” and “bottom-up” methods. The so-called top-down (physical method) method is generally accomplished by “tearing down” bulk samples and stabilizing the resulting smaller structures. An example of a top-down method process would involve the mechanical grinding of bulk metals and subsequent stabilization of the resulting nanosized metal particles by the addition of colloidal protecting agent.

The bottom-up (chemical method) methods of wet chemical nanoparticle preparation basically rely on the chemical reduction of metal salts, electrochemical pathways, or the controlled decomposition of organometallic compounds. A large variety of stabilizers, e.g., donor

ligands, polymers, and surfactants, are used in order to control the growth of the chemical reduction of transition metal salt in the presence of stabilizing agent to generate zerovalent metal colloids. Figure 3.5 illustrates these two processes.

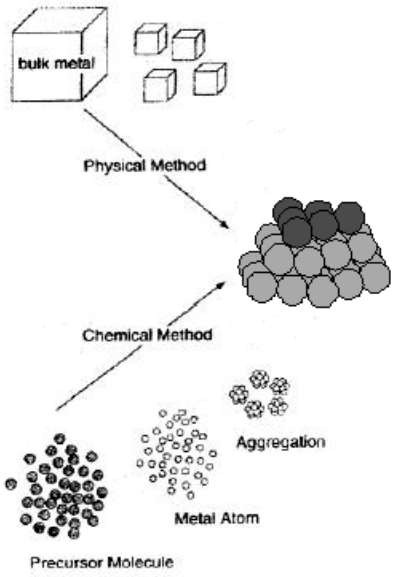

Figure 3.5. Schematic illustration of preparative methods of metal nanoclusters.

The physical methods yield dispersions where the particle size distribution is very broad. Traditional colloids are typically larger (>10 nm) and not reproducibly prepared giving irreproducible catalytic activity. Chemical methods such as the reduction of transition metal salts are the most convenient ways to control the size of the particles. Today the key goal in the transition metal nanoclusters area is the development of reproducible nanocluster synthesis in opposition to traditional colloids. Nanoclusters should be or have at least (i) specific size (1-10 nm), (ii) well-

defined surface composition, (iii) reproducible synthesis properties, (iv) isolable and redispersible.

Metal nanoclusters can be obtained by various methods leading to various particle size distributions. Nevertheless, whatever the method used a stabilizing agent is always necessary to prevent the aggregation of the colloids formed into larger particles. Five general synthetic methods are mainly used in the literature to synthesize transition metal colloids: (i) chemical reduction of transition metal salt,[40] (ii) thermal, photochemical, or sonochemical decomposition,[41] (iii) ligand reduction and displacement from organometallics,[44] (iv) metal vapor synthesis,[42] and (v) electrochemical reduction.[43]

3.3.1 Chemical Reduction Of Transition Metal Salts

The reduction of metal salts in solution is the most widely used method to generate colloidal suspensions of metals. In fact, this method is generally very simple to implement. A wide range of reducing agents have been used to obtain colloidal transition metal nanoclusters: gas such as hydrogen or carbon monoxide, hydrides or salts such as sodium borohydride or sodium citrate, or even oxidizable solvents such as alcohols.

3.3.2. Thermal, Photochemical, Sonochemical Decomposition

(i) *Thermolysis:* Many organometallic compounds are thermally decomposed to their respective zerovalent state. The synthesis of Pd and Pt organosols by thermolysis of precursors such as palladium acetate[44] or platinum halides[45] have been reported in the literature. The solvents used had high boiling points such as methyl-*iso*butylcetone. These syntheses

were performed without using stabilizing agents, and as a result, broad size distributions and large particles were observed.

(ii) *Photolysis or Radiolysis*: Photochemical synthesis of metal nanoparticles can be obtained either by (i) transition metal salt reduction by radiolytically produced reducing agents or (ii) degradation of an organometallic complex by radiolysis. The goal of these synthetic procedures is to obtain zerovalent metals under conditions, which prevent the formation of bulk metal.

(iii) Sonochemical Decomposition: The sonochemical reduction of transition metal salt occurs in three steps: the generation of the active species, the reduction of the metal, and the growth of the colloids. These three steps occur in different compartments.

3.3.3. Displacement Of Ligands From Organometallic Complexes

Some zerovalent organometallic complexes can be converted into colloidal suspension of metals by reduction or ligands displacements. Thus hydrogenation of Ru(COD)(COT) yields in the presence of either PVP, cellulose nitrate or cellulose acetate, 1 nm Ru nanoparticles.[46]

3.3.4. Condensation Of Atomic Metal Vapor

This method consists of the evaporation at reduced pressure of relatively volatile metals and a subsequent co-condensation at low temperature of these metals with the vapors of organic solvents. A colloidal dispersion of the metal was then obtained by warming the frozen metal/organic mixture. The use of metal vapors co-condensed with organic vapors to synthesized colloidal metals in nonaqueous media is known since

the dawn of the last century. However, this procedure was only extensively studied in the 70's.

3.3.5. Reduction By Electrochemical Methods

This large-scale synthetic procedure allows one to obtain size-controlled particles. A sacrificial anode is used as a metal source. This anode is oxidized in the presence of stabilizer, which is both the electrolyte and the stabilizing agent. The ions are then reduced at the cathode to yield the metallic nanoparticles. The mechanism proposed consists of (i) dissolution of the anode to form metal ions, (ii) migration of the metal ions to cathode, (iii) reduction of the metal ions at the surface of the cathode, (iv) aggregation of the particles stabilized by stabilizing agent around the metal cores then (v) precipitation of the metal nanoparticles.

3.4. Full Shell Metal Nanoclusters

Metal particles which have a complete, regular outer geometry are called full-shell or "magic number" particles. Full-shell particles are made up of concentric shells of atoms. The total number of metal atom, y, per nth shell is given by the equation $y = 10n^2+2$ ($n > 0$).[47] Thus full shell metal particles contains; 13, 55, 147, 309,… atoms as shown in Figure 2.5. Many nanoparticles' distributions center around one of these full-shell geometries. It is believed that full-shell particles posses special stability, as their closely-packed structures provide the maximum number of metal-metal bonds.[48] Control of particle size by using the ligands has been extensively studied, many shell-structured nanoparticles being synthesized, such as 2-shell Au, 4-shell Pt,[49] and 5, 7, and 8-shell Pd[50] nanoparticles.

3.5. Characterization Of Metal Nanoclusters

The properties of colloidal metal nanoparticles that are of interest include size, structure and composition. The most widely used technique for characterizing nanoparticles is transmission electron microscopy (TEM) or high resolution transmission electron microscopy (HRTEM), which provides direct visual information of the size, dispersity, structure and morphology of nanoparticles. Other commonly used methods for characterization of metal particles include UV-Visible spectroscopy (UV-Vis), nuclear magnetic resonance spectroscopy (NMR), infrared spectroscopy (IR), elemental analysis, and energy dispersive spectroscopy (EDS). To a less extent the following methods are used; analytical ultracentrifugation-sedimentation, extended X-ray absorption fine structure (EXAFS), scanning tunneling microscopy (STM), atomic force microscopy (AFM), high performance liquid chromatography (HPLC), light scattering, time of flight mass spectroscopy, magnetic susceptibility and electrophoresis or ion-exchange chromatography. Figure 3.6 gives an overall picture of the methods most commonly used in the characterization of nanoparticles.[51]

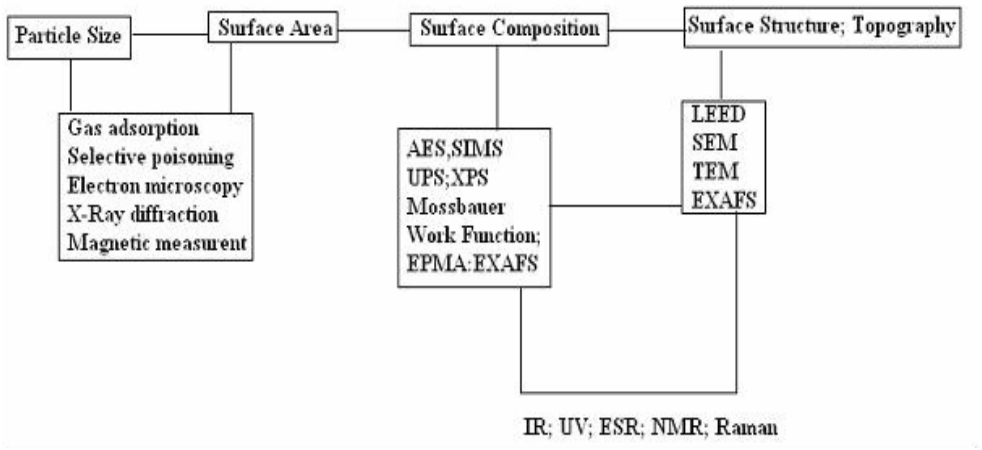

Figure 3.6. Common methods available for nanoparticles characterization.

CHAPTER 4

EXPERIMENTAL

4.1. Materials

Ruthenium(III) chloride hydrate, sodium acetate trihydrate (99%), sodium borohydride (98%), 1,2-ethane diol, toluene, ethylenediamine (99%) were purchased from Aldrich® and ethanol purchased from Merck®. Deionized water was distilled by water purification system (Şimşek SL-200, Ankara, Turkey). All glassware and Teflon coated magnetic stir bars were cleaned with acetone, followed by copious rinsing with distilled water before drying at 150 °C for a few hours.

4.2. Preparation Of Acetate Stabilized Ruthenium(0) Nanoclusters

Acetate stabilized-Ru(0) nanoclusters were prepared by following the procedure given in the literature,[52] 1.0 mL of 1.0 M aqueous sodium acetate (136.1 mg $CH_3CO_2Na.3H_2O$) solution was added to 10 mL of 2.0 mM aqueous $RuCl_3.xH_20$ (4.2 mg $RuCl_3.xH_20$) solution and under vigorous stirring, 1.0 mL of 0.11 M of aqeous $NaBH_4$ (4.3 mg $NaBH_4$) solution was introduced dropwise to prepare Ru(0) hydrosol in which acetate served as the stabilizer. A molar ratio of $NaBH_4$ to $RuCl_3$ greater than 5 was used to

ensure complete reduction of Ru to its zerovalent state. Ru hydrosol thus obtained was dark brown in color and very stable. No precipitation occurred after six days of storage.

4.3. Preparation Of Acetate/Dodecanethiol Stabilized Ruthenium(0) Nanoclusters

Acetate/dodecanethiol-stabilized ruthenium(0) nanoclusters were prepared by following the general procedure given in the literature,[53] 67.4 mg $RuCl_3.xH_20$ (3.25 mM) and 680 mg $CH_3CO_2Na.3H_2O$ (50 mM) were dissolved in 100 mL of 1,2-ethanediol. This solution was heated to 170 $^{\circ}$C for 10 min with stirring. At this temperature the colour of the solution turned from intense red to pale green and finally to brown, indicating the reduction of Ru^{3+} to Ru^0. Ruthenium(0) particles were separated from polyol either by centrifugation or by extraction in toluene solution of dodecane thiol. Reactions are considered to be quantitative when the recovered ethylene glycol is colorless (a pale green ethylene glycol indicates that the presence of unreduced Ru(II) species).

Ru particles prepared in a hydrophilic medium (ethylene glycol) were extracted into a 0.6 mL dodecane thiol (32.5 mM) solution in toluene (100mL). Polyol and toluene are immiscible at room temperature, and migration of the metal particles toward the hydrophobic phase is complete provided that the thiol/Ru molar ratio is high enough, namely higher than 0.1 (we adjusted this ratio equals to 1). To favor separation of these two phases, distilled water was added to the polyol. Finally colloidal solution containing dodecane thiol stabilized-ruthenium(0) nanoparticles in toluene were prepared.

4.4. Preparation Of Ethylenediamine Stabilized Ruthenium(0) Nanoclusters

According to a typical experiment,[54] 0.1 mL ethylenediamine was added dropwise to 20 mL of 2.0 mM stirred aqueous solution of $RuCl_3.xH_20$. Stirring was continued for five minutes after the end of the addition. A black precipitate was formed, this black solid was spun down in a centrifuge and the supertanant liquid was discarded. The black precipitate thus obtained was dissolved in 30 mL of ethanol. To this solution, 1 mL of freshly prepared 0.1 M aqeous solution of $NaBH_4$ was added dropwise under constant vigorous stirring. Stirring was continued for three minutes at the end of the addition, thereafter the ruthenium(0) nanoparticles salted out as black precipitate. The ruthenium(0) nanoclusters were centrifuged and rinsed twice with a 30 % (v/v) water/ethanol mixture to remove any unbound ethylenediamine and inorganic (Na, Cl, B) impurities. The cleaned precipitates were then dried under vacuum. Ruthenium(0) nanoclusters thus obtained readily dispersed in water.

4.5. Catalytic Activity Of Ruthenium(0) Nanoclusters In The Hydrolysis Of Sodium Borohydride

In a series of experiments, acetate, acetate/dodecanethiol, or ethylenediamine stabilized-ruthenium(0) nanoclusters were tested for their catalytic activity in the hydrolysis of sodium borohydride, to select the best stabilizing agent for this catalytic reaction. The catalytic activity of ruthenium(0) nanoparticles in the hydrolysis of sodium borohydride was determined by measuring the rate of hydrogen generation.

Before starting the catalytic activity test, a 75 mL reaction flask with jacket containing a Teflon-coated stir bar was placed on a magnetic stirrer

(Heidolph MR-301) and thermostated to 25 °C by circulating water through its jacket from a constant temperature bath. Then, a graduated glass tube (50 cm in height and 2.5 cm in diameter) filled with water was connected to the reaction flask to measure the volume of the hydrogen gas to be evolved from the reaction. Next, 284 mg (7.5 mmol) $NaBH_4$ was dissolved in 40 mL water and the solution was transferred with a 50 mL pipette into the reaction flask thermostated at 25 °C. Then, 10 mL aliquots of 2.0 mM ruthenium(0) nanoclusters' solutions stabilized by acetate, acetate/dodecanethiol, and ethylenediamine was transferred into the reaction flask using a 10 mL gastight syringe. The initial concentrations of $NaBH_4$ and ruthenium(0) nanoclusters were 150 and 0.40 mM, respectively. The experiment was started by closing the reaction flask and turning on the stirring at 1000 rpm simultaneously. The volume of hydrogen gas evolved was measured by recording the displacement of water level every 30 seconds. The reaction was ceased when 70% conversion was achieved.

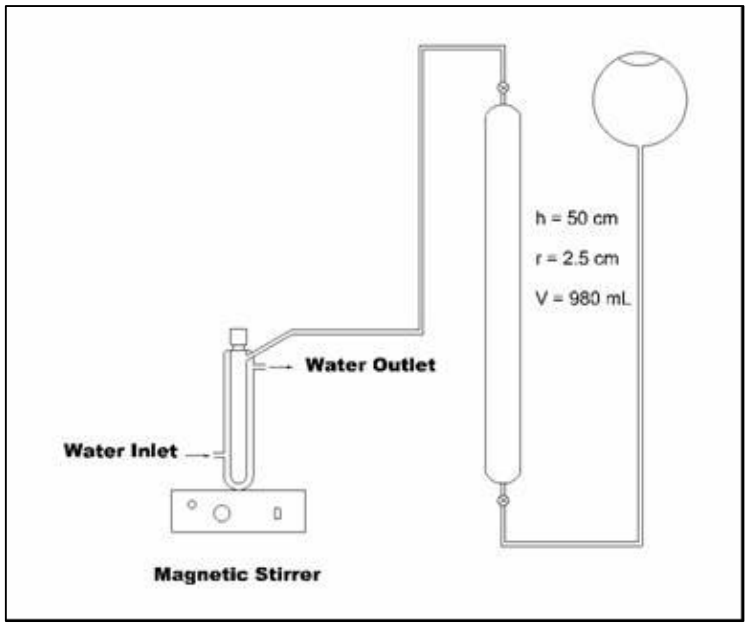

Figure 4.1. The experimental setup used in measuring the hydrogen generation rate.

4.6. Self Hydrolysis Of Sodium Borohydride

In order to test the hydrolysis of sodium borohydride in the absence of suitable catalyst, 284 mg (7.5 mmol) sodium borohydride was dissolved in 50 mL water and the solution was transferred with a 50 mL pipette into the reaction flask thermostated at 25 $^{\circ}$C. The experiment was started by closing the reaction flask and turning on the stirring at 1000 rpm simultaneously. The volume of hydrogen gas generated was recorded every 30 seconds.

4.7. TEM (Transmission Electron Microscopy) Analysis Of Acetate Stabilized-Ruthenium(0) Nanoclusters

TEM Sample Preparation: The samples used for the TEM experiments were harvested from the preparation of acetate stabilized-ruthenium(0) nanoclusters solution as described above: 5 mL aliquot of acetate stabilized-ruthenium(0) nanoclusters' solution was transferred into a clean screw-capped glass vial with a disposable polyethylene pipette. This sample was sent to the University of Oregon for TEM investigation. There, one drop of the colloidal solution was dispersed on the chloroform cleaned, carbon coated Cu transmission electron microscope grid and the solvent was then evaporated.

TEM Analyses: TEM Analyses were performed at the University of Oregon with expert assistance of Dr. Eric Schabtach, using the sample preparation procedure and Philips CM-12 TEM with a 70 μm lens operating at 100kV and with a 2.0 Å point-to-point resolutions. Samples were examined at magnification between 100 and 400K.

Particle Size Measurements: Particle size analysis was performed using the public domain NIH Image J 1.62 program[55] developed at the U.S.

National Institutes of Health and available on the Internet at http://rsb.info.nih.gov/nih-image/. The image was obtained as a TIF file directly from the TEM measurement. Using Adobe Photoshop the contrast and brightness and channel curves were adjusted so that particles stand out clearly from the background. In NIH Image J 1.62, after having set the scale and the threshold, the analyze particles feature was used to generate a table of particle areas and diameters (major and minor axes). This table was then exported into Microsoft Excel XP where histograms, statistical analysis and histogram plotting were performed. For each particle, the diameter was calculated from the area by assuming that the nanoclusters are circular. Size distributions are quoted as the mean diameter ± the standart deviation.

4.8. XPS (X-Ray Photoelectron Spectroscopy) Analysis Of Acetate Stabilized-Ruthenium(0) Nanoclusters

XPS Sample Preperation: Briefly, 10 mL of aliquots of acetate stabilized-ruthenium(0) nanoclusters' solutions were transferred via disposable pipet into eight new 15×100 mm glass tubes separately and all the samples were simultaneously centrifuged for 3 hours, and were rinsed thrice with a 30% (v/v) water/ethanol mixture to remove water soluble impurities. Next, the precipitates were dried under vacuum for 2 hours. The dried nanoclusters' samples were collected in a screw-capped glass vial and sent to the Colorado State University for XPS analysis.

XPS Analysis: X-ray photoelectron spectroscopy (XPS) was taken at the Colorado State University using a Physical Electronics 5800 spectrometer equipped with a hemispherical analyzer and using monochromatic Al-Kα radiation (1486.6 eV, the X-ray tube working at 15 kV and 350 W) and pass energy of 23.5 eV.

4.9. FTIR Analysis Of Acetate Stabilized-Ru(0) Nanoclusters

The sample prepared for the XPS analysis was also used for the FTIR analysis. FTIR spectrum of the acetate stabilized-ruthenium(0) nanoclusters was taken from KBr pellet on a Nicolet 510 FTIR Spectrophotometer using Omnic software.

4.10. Kinetic Study Of Ruthenium(0) Nanoclusters Catalyzed Hydrolysis Of Sodium Borohydride

In order to establish the rate law for the catalytic hydrolysis of $NaBH_4$ using water-dispersible Ru(0) nanoclusters, two different sets of experiments were performed at 25 $^{\circ}$C in the same way as described in the section 4.5 "Catalytic Activity Test of Ruthenium(0) Nanoclusters In The Hydrolysis of Sodium Borohydride". In the first set of experiments, the concentration of $NaBH_4$ was kept constant at 150 mM, and the Ru(0) nanoclusters' concentration was varied in the range of 0.10, 0.20, 0.40, 0.60, 0.80, 1.0 and 1.4 mM. In the second set of experiments, Ru(0) nanoclusters' concentration was held constant at 0.40 mM while the $NaBH_4$ concentration was varied in the range of 40, 80 and 200 mM to get various $NaBH_4$ / Ru(0) ratios ($NaBH_4$ / Ru(0) = 100, 200, and 500). Finally, we performed the catalytic hydrolysis of $NaBH_4$ in the presence of Ru(0) nanoclusters at constant $NaBH_4$ and Ru(0) concentrations at various temperatures in the range of 30, 35, 40 and 45 $^{\circ}$C in order to obtain the activation energy (E_a), enthalpy of activation ($\Delta H^{\#}$) and entropy of activation ($\Delta S^{\#}$).

4.11. Effect Of Acetate Concentration On The Catalytic Activity Of Ruthenium(0) Nanoclusters

In order to understand the effect of acetate concentration on the catalytic activity of Ru(0) nanoclusters in the hydrolysis of sodium borohydride (150 mM), six experiments were performed starting with various concentrations of sodium acetate (0.50, 0.80, 1.0, 1.5, 2.0 and 10 M) in the preparation of 0.4 mM Ru(0) nanoclusters. In all sets total volume of solution was kept constant at 50 mL.

4.12. Effect Of Sodium Hydroxide On The Ruthenium(0) Nanoclusters Catalyzed Hydrolysis Of Sodium Borohydride

There is no self hydrolysis of sodium borohydride in the alkaline medium. In strongly alkaline solution, $NaBH_4$ does not undergo hydrolysis to produce H_2 in appreciable amount, in the absence of suitable catalyst. In order to test the stabilizing effect of NaOH, hydrolysis of sodium borohydride (150mM) was carried out in 10% (w/w) NaOH solution in the absence of ruthenium(0) nanoclusters and it was observed that there is no considerable amount of hydrogen production over one day. A critical reexamination of the literature showed us the catalytic activitiy of some heterogeneous catalysts in the hydrolysis of sodium borohydride have been investigated in the alkaline solution (<10 % NaOH). Then, in order to compare the catalytic activity of these catalyts with ruthenium(0) nanoclusters we performed the catalytic activity test of ruthenium(0) nanoclusters for the hydrolysis of sodium borohydride in aqeous solution containing 10% NaOH (w/w), exactly in the same way as described above. Hydrolysis of sodium borohydride (150 mM) in the presence of ruthenium(0) nanoclusters (0.40 mM) in 10% NaOH (w/w) solution was performed at different temperatures 25, 35, 45, and 55 $^{\circ}$C.

4.13. Mercury Poisoning Of Acetate Stabilized Ruthenium(0) Nanoclusters

To determine the true number of catalytically active surface sites of catalyst, the acetate stabilized ruthenium(0) nanoclusters were poisoned by mercury which blocks the active sites of catalyst. For this experiment 1.0 mM ruthenium(0) nanoclusters used in the hydrolysis of 150 mM sodium borohydride (54.8 mg) in 10 mL solution poisoned by 0.10, 0.22, 0.33, 0.67 and 3.3 mg of mercury (mol Ru(0) / mol Hg = 300, 200, 100, 50 and 10) respectively and the rate of hydrogen generation measured.

4.14. The Catalytic Lifetime Of Acetate Stabilized Ruthenium(0) Nanoclusters

The catalytic lifetime of ruthenium(0) nanoclusters in the hydrolysis of sodium borohydride was expressed as total turnover number, for this purpose 0.333 mM Ru(0) nanoclusters were used in the hydrolysis of 450 mM (851 mg) $NaBH_4$. At the end of the reaction by considering the total volume of generated H_2 and the reaction time the total turnover number (TTON) of acetate stabilized ruthenium(0) nanoclusters were calculated.

4.15. Bottlability (Isolability And Reusability) Of Acetate Stabilized Ruthenium(0) Nanoclusters

The prepared acetate stabilized ruthenium(0) nanoparticles were centrifuged and rinsed thrice with a 30% (v/v) water/ethanol mixture to remove inorganic impurities (Na, Cl, B). The cleaned precipitates were dried under vacuum. Then these isolated ruthenium(0) nanoclusters were redispersed in water and their catalytic activities were tested in the hydrolysis of sodium borohydride.

CHAPTER 5

RESULTS AND DISCUSSION

5.1. Synthesis Of Water Soluble-Ruthenium(0) Nanoclusters

The proposed mechanism for the stepwise formation of ruthenium(0) nanoclusters is based on the nucleation, surface growth and agglomeration.[56] The ruthenium salt is reduced to give zerovalent ruthenium atoms in the embryonic stage of nucleation which can collide in the solution with further ruthenium ions, ruthenium atoms or ruthenium clusters to form an irreversible "seed" of stable ruthenium nuclei.

The nuclei growth during the "ripening" process gives colloidal ruthenium particles in nm size range. The mechanism for the particle formation is an agglomeration of zerovalent nuclei in the "seed" or alternatively collisions of already formed nuclei with reduced ruthenium atoms.

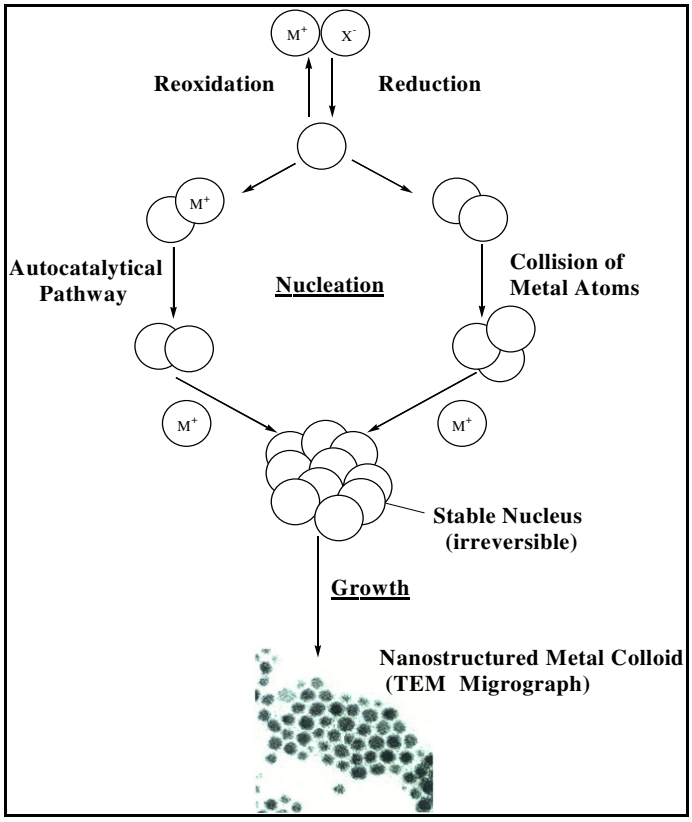

Figure 5.1. Formation of ruthenium colloids via the "salt reduction" method. (Taken from the literature[57]).

Three different methods were followed for the synthesis of ruthenium(0) nanoclusters, each starting with $RuCl_3.xH_20$ as metal precursor. Stable colloidal solutions of ruthenium(0) nanoclusters were obtained by the reduction of $RuCl_3.xH_2O$ in polyol for acetate/dodecanethiol stabilized ruthenium nanoclusters, in water for acetate stabilized ruthenium(0) nanoclusters and in ethanol for ethylenediamine stabilized ruthenium(0) nanoclusters, respectively.

In the preparation of ethylenediamine stabilized ruthenium(0) nanoclusters when ethylenediamine was introduced to the aqueous solution of $RuCl_3.xH_2O$ with stirring a black precipitate appeared within a very short

time. The exact structure of this solid is not known at present, although a structure similar to the one given in Figure 5.2 may be proposed based on the report of Broomhead and Maguire[58] in 1967.

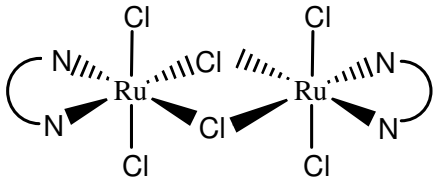

Figure 5.2. Proposed structure of $RuCl_3$-(en) complex.

The ruthenium(0) nanoclusters, obtained by the current procedure can be easily dispersed in water and giving rise to a transperent dark brown colloidal solution of ruthenium. This colloidal solution displays good stability. No precipitation was visible even after storage for two weeks. In the synthesis of acetate/dodecanethiol stabilized ruthenium(0) nanoclusters acetate provides electrostatic stabilization in ethylene glycol and dodecanethiol provides steric stabilization in toluene. Generally reduction of metal salts in liquid polyols has proven to be suitable method for the synthesis of monodisperse metal particles in the nanometer size range. In this method the ethylene glycol act as solvent for the ruthenium salt, reducing agent, and growth medium for the ruthenium particles. Actually in this procedure dodecanethiol was used as phase transfer reagent but it's strongly believed that it acts also as stabilizing agent by forming a protective layer around ruthenium atoms. For this reason we observed that acetate/dodecanethiol stabilized ruthenium(0) nanoclusters are more stable than both acetate and ethylenediamine stabilized ruthenium(0) nanoclusters. The colloidal solution has excellent stability and precipitation was not observed even after one month storage.

The only acetate stabilized Ru(0) nanoparticles were prepared by the $NaBH_4$ reduction of $RuCl_3.xH_20$ in water at room temperature. In this method without the addition of sodium acetate, the ruthenim(0) nanoclusters would easily agglomerate and precipitate out from the solution. In the presence of sodium acetate precipitation was not observed even after several days of storage, demonstrating the role of acetate as a stabilizer. The adsorption of acetate anions on ruthenium(0) nanoparticles and the resulting electrostatic repulsion between the nanoparticles had adequately prohibited the latter from getting close enough for irreversible particle growth. In addition to simplicity of acetate stabilization of ruthenium(0) nanoclusters, the acetate adsorbed on the surface of the ruthenium(0) nanoclusters could be easily displaced by stronger coordinating ligands serving as replacement stabilizers. This property makes the acetate stabilized ruthenium(0) nanoclusters a good starting material for constructing complex ruthenium(0) clusters by using the same Ru core particles and by exchanging acetate with stronger and multifunctional stabilizing agents.

5.2. The Catalytic Activity Of Ruthenium(0) Nanoclusters $[Ru(0)]_nL_x$

In order to decide which stabilizing agent provides highest catalytic activity to ruthenium(0) nanoclusters in the hydrolysis of sodium borohydride, several sets of experiments were performed in the presence of three different stabilizing agents; acetate, dodecanethiol and ethylenediamine. In all experiments, catalytic activity was measured by monitoring the rate of hydrogen generation in the catalyzed hydrolysis of sodium borohydride. Figure 5.3 shows the catalytic activities of three different catalysts acetate, acetate/dodecanethiol and ethylenediamine stabilized ruthenium(0) nanoclusters.

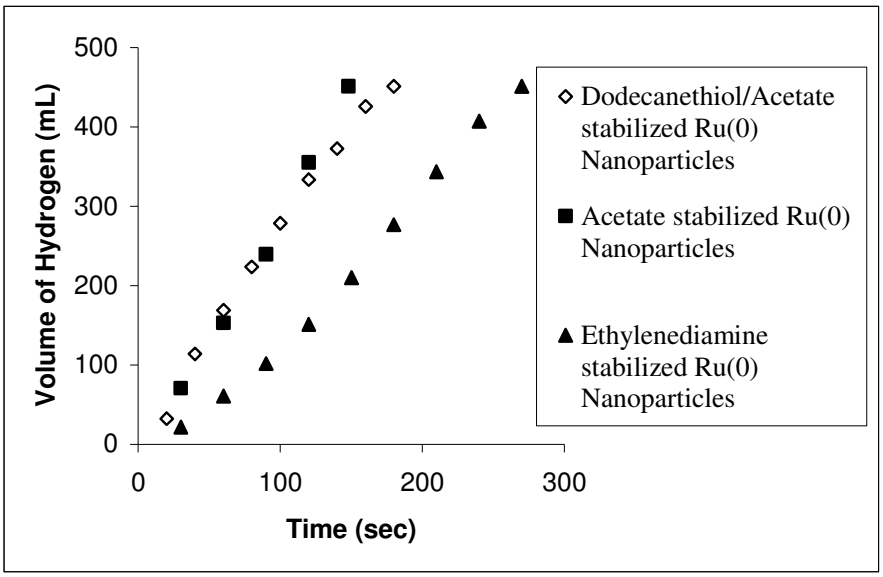

Figure 5.3. The catalytic activity of $[Ru(0)]_nL_x$ (L = ethylenediamine, acetate/dodecanethiol, acetate) in the hydrolysis of sodium borohydride.

The highest catalytic activity was obtained by using acetate anion as stabilizing agent. The reason why only the acetate stabilized ruthenium(0) nanoparticles are more active catalyst in the hydrolysis of sodium borohydride compared to acetate/dodecanethiol stabilized ruthenium(0) nanoparticles can be explained by the presence of dodecanethiol since the long chain of dodecanethiol can block the active sites of catalyst but also provides high stability. After these experiments, the only acetate-stabilized ruthenium(0) nanoclusters were selected to be used in catalyzing the hydrolysis of sodium borohydride. However, it had to be characterized before using as catalyst.

5.3. Characterization Of Acetate Stabilized-Ru(0) Nanoparticles

The acetate stabilized ruthenium(0) nanoclusters were characterized by X-ray photoelectron spectroscopy (XPS), transmission electron microscopy (TEM) and FT-IR spectroscopy.

5.3.1. X-Ray Photoelectron Spectroscopy Analysis

In analyzing of XPS spectrum of ruthenium nanoclusters we used the reference values shown in Table 5.1. The XPS spectrum of acetate stabilized ruthenium(0) nanoclusters exhibit 2 prominent signals at 280 and 463 eV for ruthenium. Unfortunately, the intense C 1s peaks at 285 eV suppress the Ru 3d3/2 peak expected in the same region. However, the weak feature at 280 eV can be assigned to the Ru 3d5/2 signal for the zero valence state as shown in Figure 5.4.

Table 5.1. Line positions of ruthenium atom in X-ray photoelectron spectrum of metallic ruthenium.[59]

Photoelectron Lines of Ruthenium	
	Binding Energy
3s	586 eV
$3p_{1/2}$	484 eV
$3p_{3/2}$	462 eV
$3d_{5/2}$	280 eV
4s	75 eV
4p	43 eV

In addition to Ru $3d_{5/2}$ signal at 280 eV, the signal of Ru $3p_{3/2}$ at 462 eV corresponds to Ru zerovalent state, shown in Figure 5.5. The signal around 464 eV can be assigned to higher oxidation states of ruthenium such as Ru(IV) in RuO_2. This can be formed from the oxidation of ruthenium(0) nanoparticles during XPS sampling procedure.

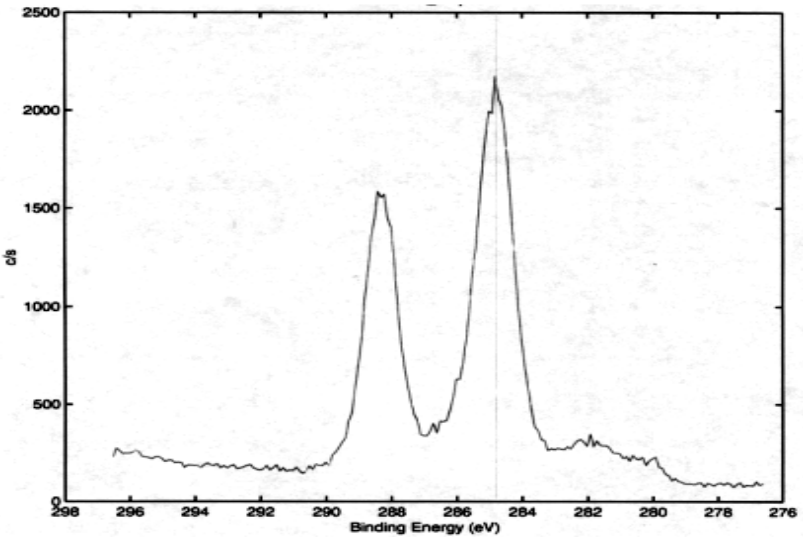

Figure 5.4. X-ray photoelectron spectrum of acetate stabilized-Ru(0) nanoparticles, in the region of 276-296 eV.

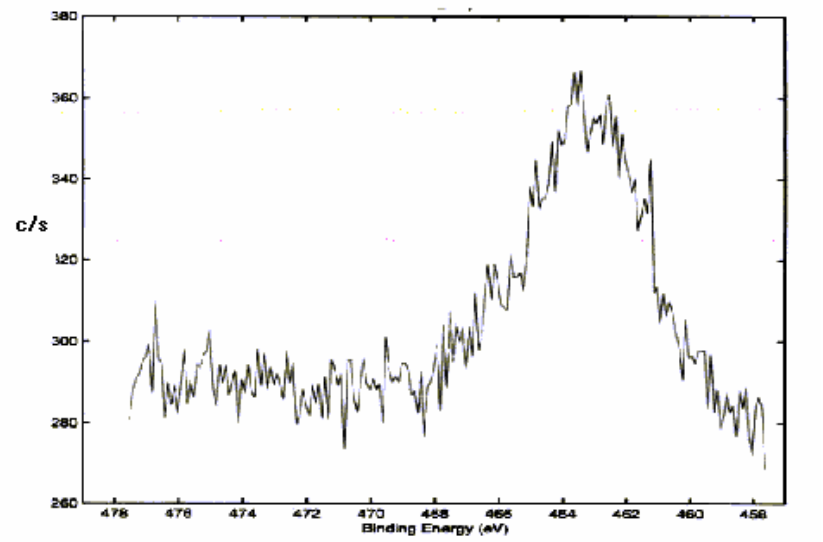

Figure 5.5. X-ray photoelectron spectrum of acetate stabilized-Ru(0) nanoparticles in the region of 458-478 eV.

5.3.2. Transmission Electron Microscopy Analysis

The TEM image of ruthenium(0) nanoclusters is given in Figure 5.6.(a). This TEM image was used to analyze the particle size and size distribution of ruthenium(0) nanoparticles using NIH image program. Figure 5.6 (b) gives the NIH images of acetate stabilized ruthenium(0) nanoparticles. For each particle the diameter was calculated from the area by assuming that nanoparticles are circular.

(a)

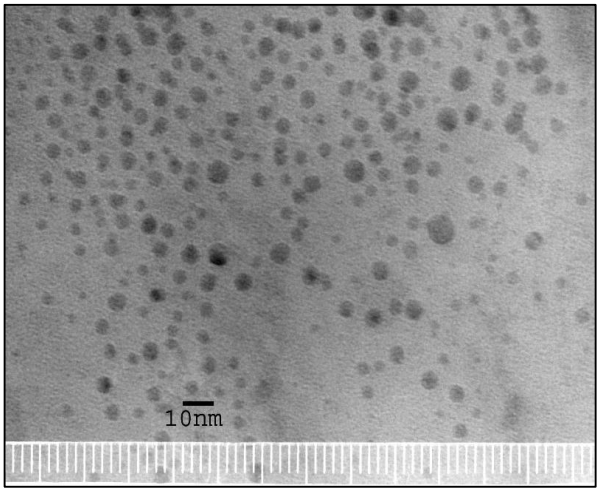

(b)

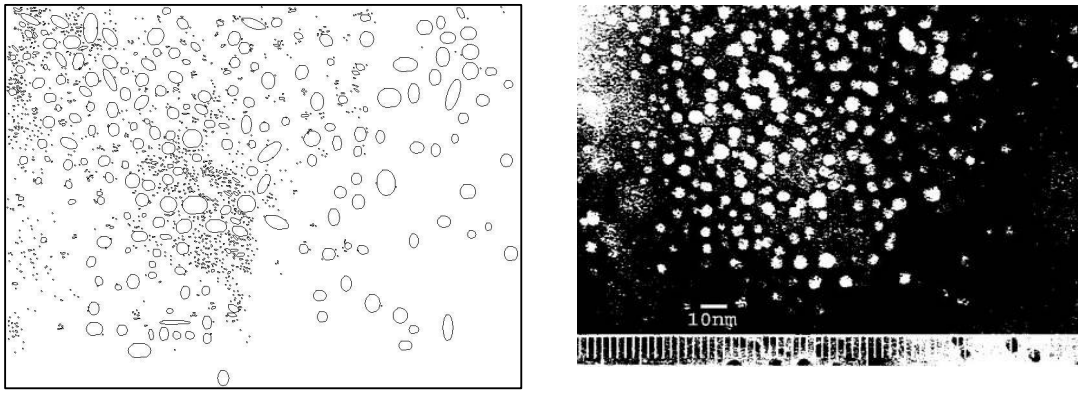

Figure 5.6. (a) TEM image, **(b)** NIH images of acetate stabilized ruthenium(0) nanoclusters.

Figure 5.7 shows the histogram of acetate stabilized ruthenium(0) nanoclusters, drawn by using the data obtained from the analysis of the TEM image in Figure 5.6. The histogram contains the size of 222 non-touching particles. The particle size ranges from 1.0 to 4.4 nm with a mean value of 2.68 nm and a standart deviation of 1.12 nm.

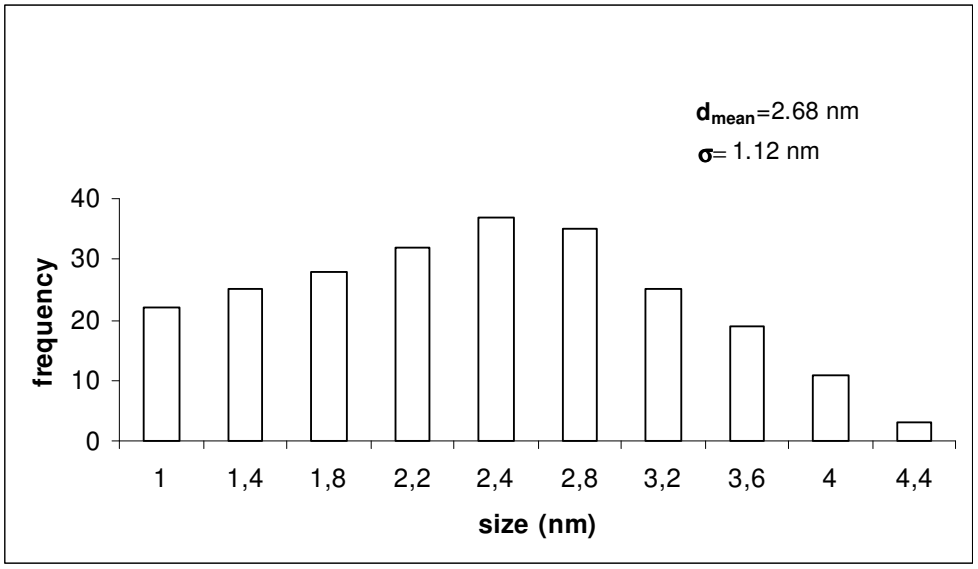

Figure 5.7. The histogram of the acetate stabilized-ruthenium(0) nanoparticles giving the number nanoparticles versus the size.

5.3.3. Infrared Spectroscopic Analysis

FT-IR spectra of the isolated ruthenium(0) nanoclusters and of the free acetate ion (in sodium acetate) are displayed together in Figure 5.8. The free acetate ion has characteristics bands at 1580 cm^{-1} and 1425 cm^{-1}. The comparison of IR spectrum of free acetate and acetate stabilized Ru(0) nanoparticles isolated shows that acetate ions exist in the nanoclusters sample most probably on the surface of particles.

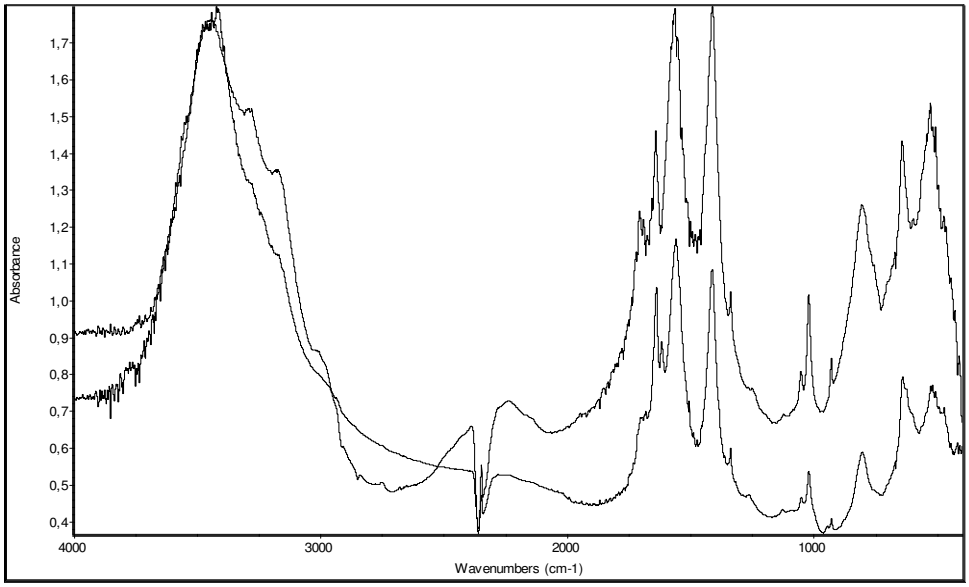

Figure 5.8. FT-IR spectra of isolated ruthenium nanoparticles (bottom curve), and free acetate anion (upper curve).

5.4. Kinetic Study Of Ruthenium(0) Nanoclusters Catalyzed Hydrolysis Of Sodium Borohydride

The kinetics of the ruthenium(0) nanoclusters catalyzed hydrolysis of sodium borohydride was studied by monitoring the hydrogen evolution depending on substrate concentration, catalyst concentration, stabilizer concentration, temperature and in the presence or absence of sodium hydroxide.

$$NaBH_4 + 2H_2O \xrightarrow{\text{Ru(0) nanoclusters}} NaBO_2 + 4H_2$$

5.4.1. The Rate Law And Activation Parameters Of Ruthenium(0) Nanoclusters Catalyzed Hydrolysis Of Sodium Borohydride

Water-dispersible ruthenium(0) nanoclusters, prepared from the reduction of ruthenium(III) chloride hydrate by sodium borohydride in water and stabilized by acetate, were used, for the first time, as catalyst in the hydrolysis of sodium borohydride liberating hydrogen gas. The ruthenium(0) nanoclusters are found to be highly active catalyst for the hydrolysis of sodium borohydride as shown in Figure 5.9, which plots the volume of generated H_2 versus time during the catalytic hydrolysis of 150 mM $NaBH_4$ solution in the presence of ruthenium(0) nanoclusters in different concentrations at 25 °C. It is seen that ruthenium(0) nanoclusters have high catalytic activity in the hydrolysis of $NaBH_4$ even at low concentrations and room temperature. The hydrogen evolution starts immediately without any induction period as a prepared catalyst is used. The hydrogen evolution rate remains constant until all the sodium borohydride is hydrolyzed. The hydrogen generation rate was determined from the linear portion of the plot for each experiment with different ruthenium(0) nanoclusters' concentrations. Figure 5.10 shows the plot of hydrogen generation rate versus ruthenium(0) nanoclusters' concentration, both in logarithmic scale. One obtains a straight line, the slope of which is found to be 1.073. It indicates that the hydrolysis is first order with respect to the concentration of ruthenium(0) nanoclusters. Figure 5.11 shows the plot of hydrogen generation rate versus $NaBH_4$ concentration, both in logarithmic scale, starting with three different initial concentrations of sodium borohydride but constant ruthenium(0) concentration at 25 °C. It is seen that the kinetics of the catalytic hydrolysis is zero order in substrate concentration, also shown in Figure 5.11. Thus, the rate law for the catalytic hydrolysis of sodium borohydride can be given as;

$$\frac{-4d[NaBH_4]}{dt} = \frac{d[H_2]}{dt} = k[Ru] \quad \textbf{(4)}$$

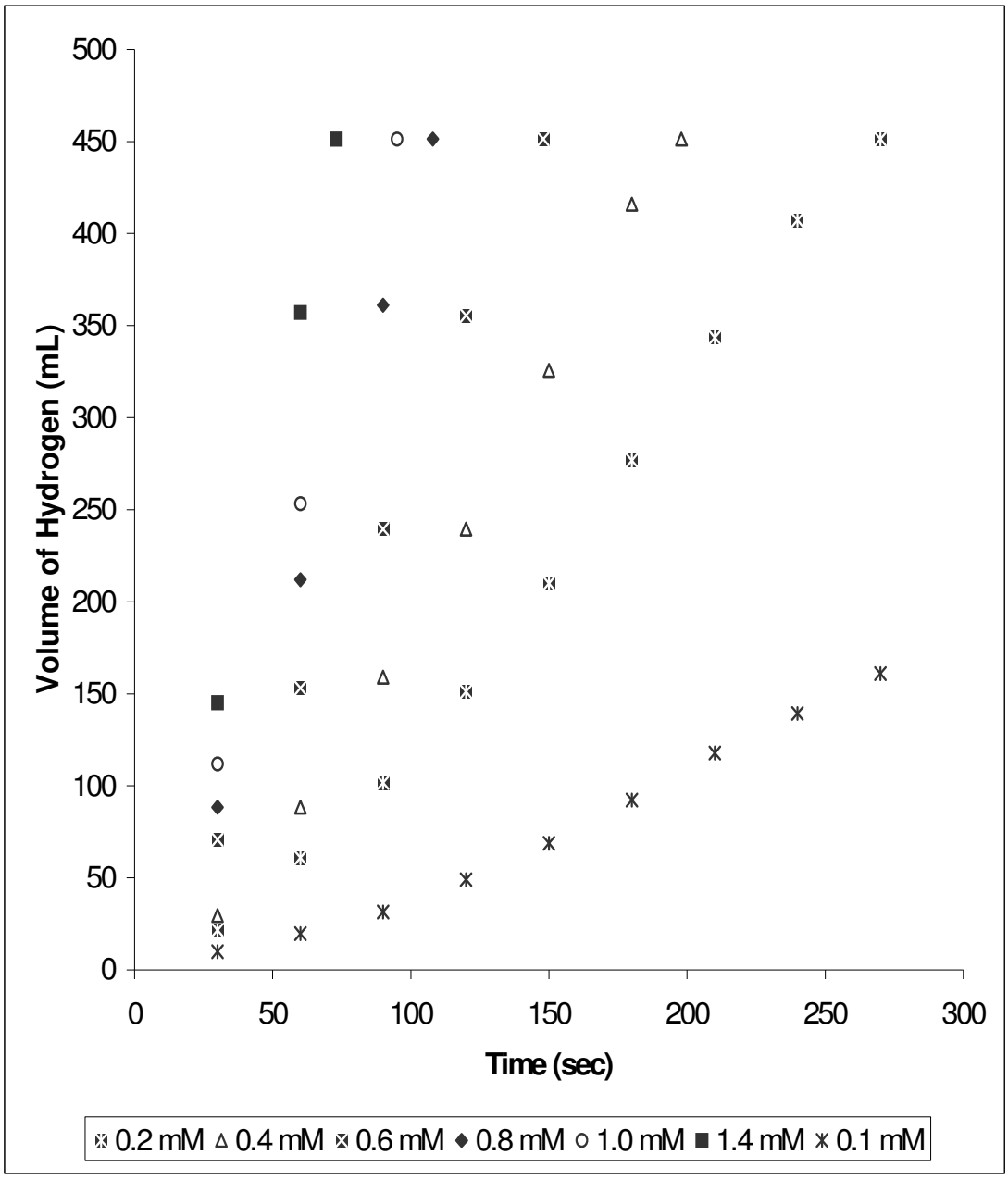

Figure 5.9. Volume of hydrogen generated versus time during the ruthenium(0) nanoparticles catalyzed hydrolysis of sodium borohydride starting with different Ru(0) concentrations.

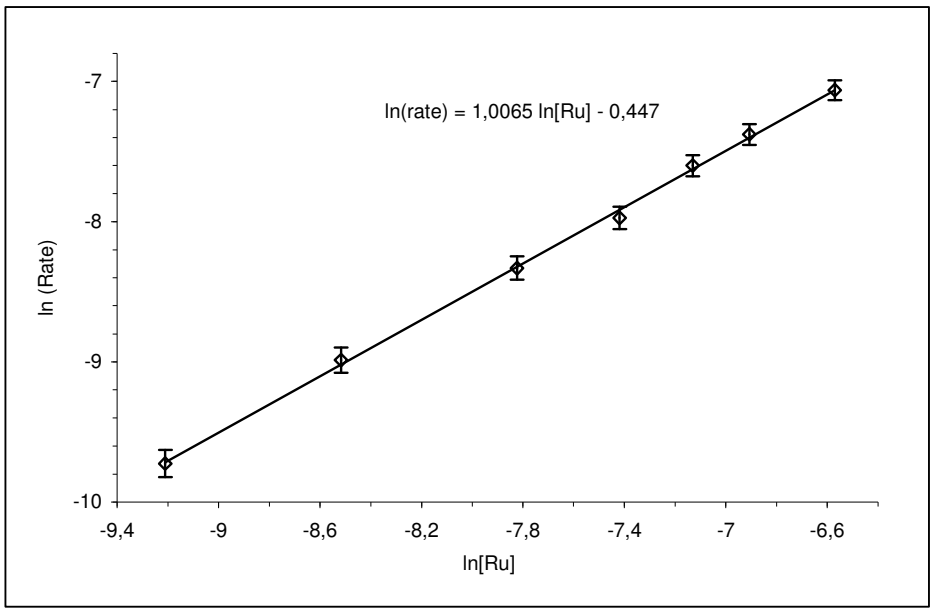

Figure 5.10. The graph of ln (rate) versus ln [Ru] for the ruthenium(0) nanoparticles catalyzed hydrolysis of sodium borohydride.

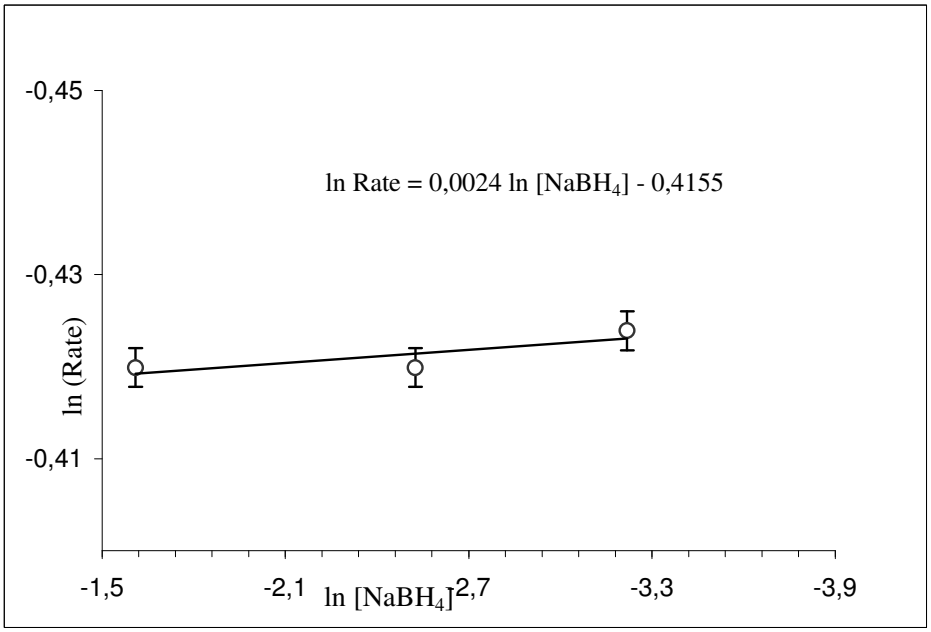

Figure 5.11. The graph of ln (rate) versus ln $NaBH_4$ ($[Ru(0)]_n$ =0,4mM in all three sets) at 25 °C.

In order to evaluate the activation parameters, ruthenium(0) nanoclusters catalyzed hydrolysis of sodium borohydride was performed at four different temperatures, 30, 35, 40, and 45°C. The values of the rate constant *k* were determined at various temperatures and listed in Table 5.2.

Table 5.2. Rate constants for the hydrolysis of sodium borohydride catalyzed by Ru(0) nanoclusters starting with a solution of 150 mM $NaBH_4$ and 0.4 mM $Ru(0)_n(acetate)_x$ nanoclusters at different temperatures.

Temperature (°C)	**Rate Constant, *k*** **([mol $NaBH_4$]·[mol Ru(0)]$^{-1}$· s^{-1})**
30	3.0
35	3.9
40	4.8
45	5.0

The rate constant / temperature data was evaluated according to the Arrhenius equation and Eyring equation to obtain the activation energy, the activation enthalpy and entropy. First, the Arrhenius equation was used for the evaluation:

$$k = A.e^{-\frac{Ea}{RT}} \quad \textbf{(5)}$$

where A and E_a are constants characteristics of the reaction and R is the gas constant. E_a is the Arrhenius activation energy and A is the pre-exponential factor.[60] Taking the natural logarithm of equation **5**, we get ;

$$\ell nk = \ell nA - \left(\frac{E_a}{RT}\right) \qquad \textbf{(6)}$$

The plot of ln k versus $\frac{1}{T}$ gives a straight line with a slope of $\left(\frac{E_a}{R}\right)$ shown in Figure 5.12.

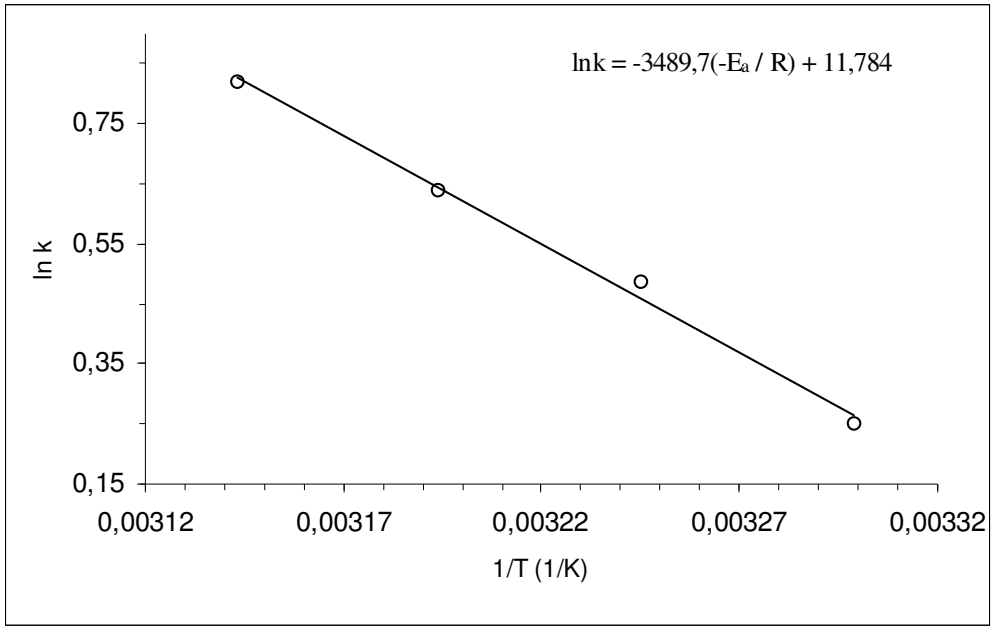

Figure 5.12. Arrhenius plot for the ruthenium(0) nanoclusters catalyzed hydrolysis of sodium borohydride at different temperatures.

From the slope of the Arrhenius plot, the activation energy, E_a, for ruthenium(0) nanoparticles catalyzed hydrolysis of sodium borohydride was calculated to be 29±2 kJ/mol.

The enthalpy of activation, $\Delta H^{\#}$ and the entropy of activation, $\Delta S^{\#}$ were calculated according to the Eyring equation **7** by drawing the graph of $\ln\frac{k}{T}$ versus $\frac{1}{T}$ given in Figure 5.13.

$$\ln\frac{k}{T} = \frac{1}{T}\left(\frac{\Delta H^{*}}{R}\right) + \ln\frac{k_b}{h} + \frac{\Delta S^{*}}{R} \qquad \textbf{(7)}$$

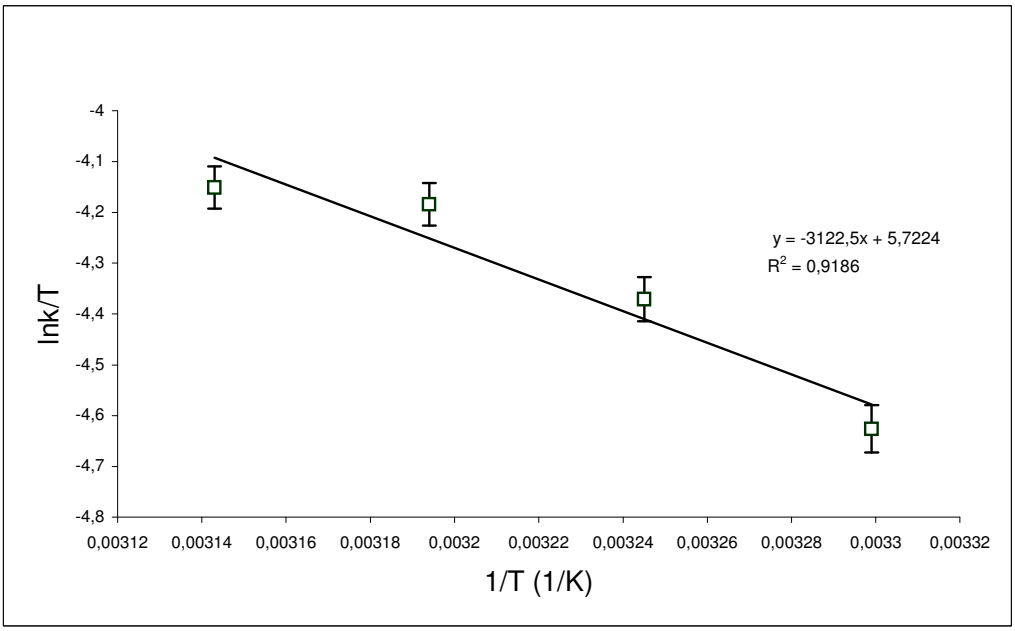

Figure 5.13. Eyring plot for ruthenium(0) nanoclusters catalyzed hydrolysis of sodium borohydride.

From the Eyring plot, the enthalpy of activation for ruthenium(0) nanoparticles catalyzed hydrolysis of sodium borohydride was calculated to be 26±1 kJ/mol, while the entropy of activation value is -150±8 J/K.mol. The small activation enthalpy and the large negative value of activation entropy are indicative of an associative mechanism for the ruthenium(0) nanoclusters catalyzed hydrolysis of sodium borohydride.

5.4.2. Ruthenium(0) Nanoclusters Catalyzed Hydrolysis Of Sodium Borohydride In The Alkaline Medium

The hydrolysis of sodium borohydride is slowed down as the pH of the solution increases.[10] Hence, there is no self hydrolysis of sodium borohydride, in the alkaline medium. Aqueous solution of sodium borohydride becomes more stable at high pH. Strongly alkaline $NaBH_4$ solutions do not produce appreciable H_2 without catalyst present. A critical review of the literature showed us, the catalytic activitiy of some heterogeneous catalysts in the hydrolysis of sodium borohydride have been reported in the alkaline solution (<10% NaOH). In order to avoid any misunderstanding about the comparison of the catalytic activity of ruthenium(0) nanoclusters with prior studies, ruthenium(0) nanoclusters catalyzed hydrolysis of sodium borohydride was performed in the alkaline medium that contains 10% NaOH (w/w). The values of the rate constant *k* of the catalytic hydrolysis of sodium borohydride in the alkaline solution were determined at various temperatures and listed in Table 5.3 and Figure 5.14 shows the Arrhenius plot. The slope of the straight line gives an activation energy of 43±2 kJ/mol for the ruthenium(0) nanoclusters catalyzed hydrolysis of sodium borohydride in alkaline solution 10% NaOH (w/w).

Table 5.3. Rate constants for the hydrolysis of sodium borohydride catalyzed by ruthenium(0) nanoclusters starting with 150 mM $NaBH_4$ and 0.4 mM ruthenium(0) nanoclusters in the alkaline solution at different temperatures.

Temperature (°C)	**Rate Constant, *k*** **([mol $NaBH_4$]·[mol Ru(0)]$^{-1}$· s^{-1})**
25	0.8
35	1.6
45	2.9
55	3.9

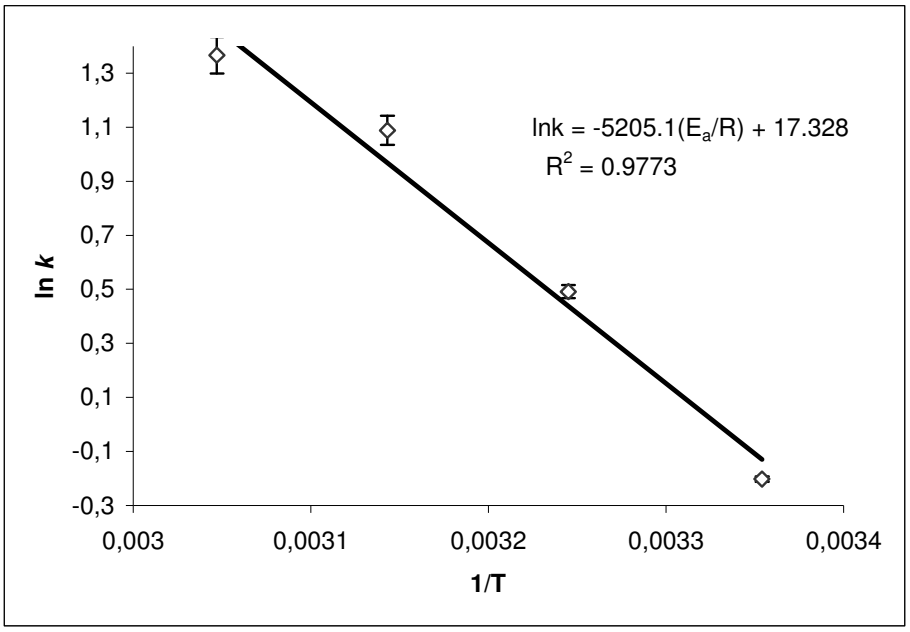

Figure 5.14. Arrhenius plot for ruthenium(0) nanoclusters catalyzed hydrolysis of sodium borohydride in the alkaline solution contains 10% NaOH (w/w).

The higher activation energy in the alkaline medium indicates that this hydrolysis reaction can be greatly inhibited by the addition of sodium hydroxide. The self-hydrolysis of sodium borohydride takes place by the reaction of borohydride ions with proton dissociated from water. In alkaline solution, the slow self-hydrolysis of $NaBH_4$ is primarily due to the reduction of proton concentration and hydroxide ions play as an inhibitor for the catalyzed $NaBH_4$ hydrolysis. Also NaOH concentration effect the activity of catalyst, because the increase in concentration of NaOH reduce the activity of water and this situation forms insoluble $NaBO_2$ which can blocks the active sites of catalyst. However in the alkaline medium again we achieved a lower activation energy than heterogeneous Ru (bulk) catalyzed hydrolysis of sodium borohydride.[2]

In non-alkaline medium using ruthenium(0) nanoclusters catalyst provides the lowest activation energy ever found for the hydrolysis of

sodium borohydride, Table 5.4 shows different catalysts with their activation energies in the hydrolysis of sodium borohydride. Also the lower activation energy was provided than that of for heterogeneous bulk Ru catalyzed hydrolysis of sodium borohydride. It is indicative that Ru(0) nanoclusters are more active catalyst than bulk ruthenium metal.

Table 5.4. The major catalysts used in the hydrolysis of sodium borohydride and the activation energies of the reaction, provided by these catalysts

Catalyst	**Activation Energy ($kJ.mol^{-1}$)**
Ruthenium(0) nanoclusters	29.2 43.3 (in alkaline medium)
Bulk ruthenium	47
Raney nickel	63
Bulk nickel	71
Bulk cobalt	75
Pt + $LiCoO_2$	97

5.4.3. Effect Of Concentration Of Sodium Acetate (OAc^-) On The Catalytic Activity Of Ruthenium(0) Nanoclusters

Another parameter in the catalytic activity of ruthenium(0) nanoclusters is the acetate concentration. It is a crucial issue to adjust the concentration of stabilizer in preparation of transition metal nanoclusters, to obtain highly active and stable nanoclusters. For this reason we performed the catalytic activity of ruthenium(0) nanoclusters in the hydrolysis of sodium

borohydride at different acetate concentrations which act as stabilizer in the formation of Ru(0) nanoparticles. Figure 5.15 shows dependence of relative rate constants of acetate stabilized Ru(0) nanoclusters catalyzed hydrolysis of sodium borohydride on acetate concentration. We observed that the highest catalytic activity can be achieved by using 1.0 M acetate (approximately 50 times of $RuCl_3$ concentration) in the synthesis of acetate stabilized Ru(0) nanoparticles.

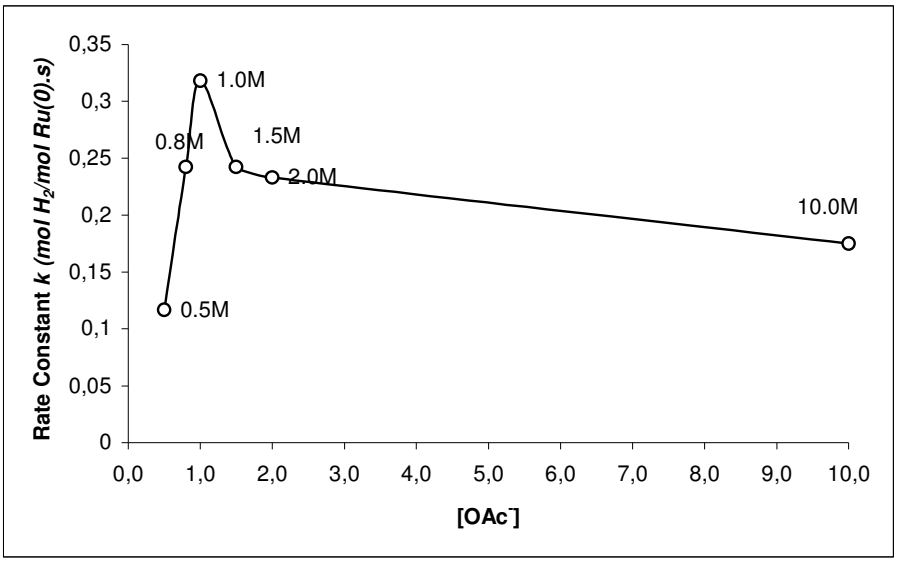

Figure 5.15. Relative rate constants of acetate stabilized-Ru(0) nanoparticles catalyzed hydrolysis of sodium borohydride versus different acetate concentrations.

5.4.4. Mercury Poisoning Experiment

A determination of percentage of catalytically active surface metal atoms in the ruthenium(0) nanoclusters is another important issue. Catalyst poisoning kinetics are an essential component of any study that aspires to establish the true number of active sites or any property connected to this value such as the turnover frequency (TOF) or total turnovers (TTO's). In

order to find the true number of catalytically active surface sites of catalyst, the acetate stabilized ruthenium(0) nanoclusters were poisoned by mercury when it catalyzed the hydrolysis of sodium borohydride. Figure 5.16 shows the results of eight independent experiments, plotted as the relative rate versus the moles of Hg/the moles of total Ru(0). Linear poison plots, such as the one in Figure 4.13, have been reported in the literature and are readily described by a simple line, equation **8**, [61] where y is the relative rate, $-m$ is the slope of the line ($m>0$), and x is the moles of Hg/moles of total Ru.

$$y = -mx + y_{\text{intercept}} \qquad \textbf{(8)}$$

The amount of Hg required to completely poison the catalyst is indicated by the intersection of the poison plot with the x-axis, that is at $y = 0$. To determine the value of $x_{\text{intercept}}$, a linear regression analysis of the resulting slope and $y_{\text{intercept}}$ were used to calculate the $x_{\text{intercept}}$ from equation **9** obtained when $y = 0$.

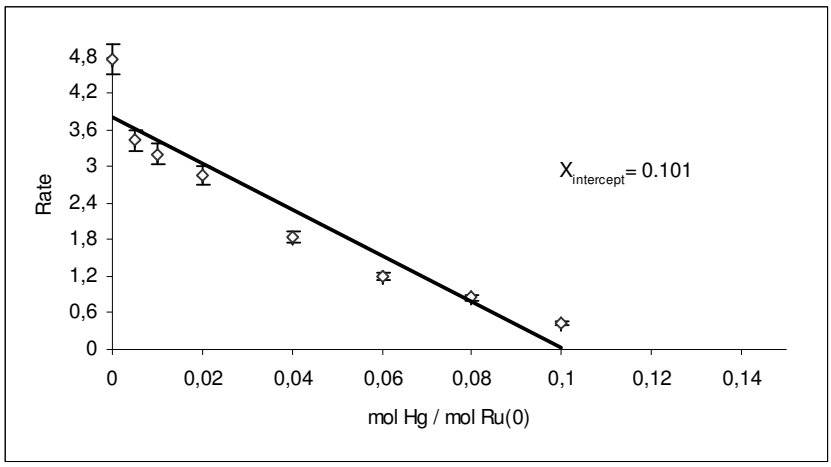

Figure 5.16. Plot of relative rate of hydrolysis of sodium borohydride versus moles of Hg/moles of total Ru(0) for the hydrolysis of sodium borohydride by 2.68 ±1.12 nm ruthenium(0) nanoclusters.

$$x_{intercept} = y_{intercept} / m \qquad \textbf{(9)}$$

The $x_{intercept}$ of the plot in Figure 5.16 is 0.101 ± 0.05 mol of Hg / mol of total ruthenium(0) nanoclusters present, states that only 10% mol of Hg is sufficient to poison completely all of the available active sites of the ruthenium(0) nanoclusters.

5.4.5. Determination Of Surface Active Atoms In Ru(0) Nanoparticles

The number of ruthenium atoms per each cluster was calculated by using TEM results that gave us the mean diameter of ruthenium(0) nanoparticles. First of all considering TEM results the mean diameter of ruthenium(0) nanoparticles was found to be 2.68±1.12 nm then we assumed that ruthenium(0) nanoclusters form hexagonal close packed structure in which the unoccupied space amounts to 26 % of the total volume and the atomic radius of ruthenium atom (0.134 nm) the number of ruthenium(0) atoms per each cluster was calculated as follows;

$$\text{r (mean)} = \frac{2.68}{2}\text{nm} = 1.34\,\text{nm}$$

$$\text{N} = \frac{\text{V (nanocluster)}}{\text{V (atom)}} = \frac{(0.74)\frac{4}{3}\pi\,(\text{r}_{\text{mean}})^3}{\frac{4}{3}\pi\,(\text{r}_{\text{atom}})^3} = 0.74\left[\frac{1.34\,\text{nm}}{0.134\,\text{nm}}\right]^3$$

$$\text{N} \cong 740\ \text{Ru(0) atoms per cluster}$$

According to Schmid's formula[27] (equation **10**) the number of metal atoms, *y,* per *n*th shell, in a full shell "magic number" cluster can be calculated. Figure 5.17 presents the idealized hexagonal close-packed full-shell "magic number" clusters.

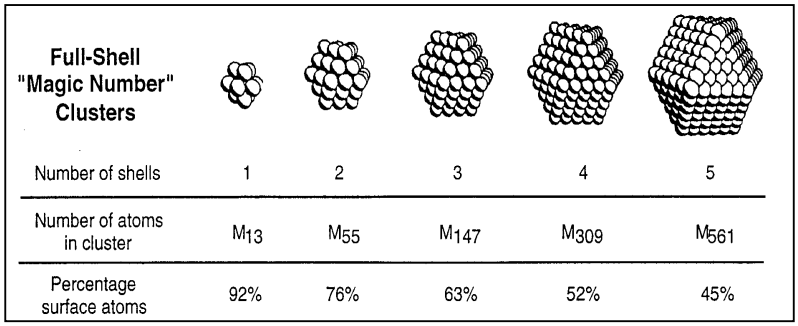

Figure 5.17. The idealized presentation of hexagonal close-packed full-shell "magic number" clusters. Each metal atom has the maximum number of nearest neighbours, which imparts some degree of extra stability to full-shell clusters. The percentage of surface atoms decreases as the number of atoms increases.(taken from literature[21(c)]).

$$y = 10n^2 + 2 \quad (n > 0) \qquad \textbf{(10)}$$

Under the consideration of this formula the percentage of surface atoms for Ru(0) nanoclusters was found to be in the interval of 45% and 39% given in Table 5.4. In other words 39-45 % of total ruthenium atoms are on the surface of Ru(0) nanoclusters. If we consider only the mean value, it gives us 42 % of total ruthenium atoms present on the surface of Ru(0) nanoclusters.

Table 5.5. The number of total ruthenium(0) atoms in cluster, surface ruthenium(0) atoms and their percentage for different shells. (n= number of shell, N= number of atoms in cluster, N_s= number of surface atoms in nanocluster, d= mean diameter of ruthenium atoms required to form this nanoclusters).

n	N	N_s	d[nm]	% surface atoms
1	13	12	0,70	92
2	55	42	1,13	76
3	147	92	1,56	63
4	309	162	2,00	52
5	**561**	**252**	**2,44**	**45**
6	**923**	**362**	**2,88**	**39**
7	1415	492	3,33	35
8	2057	642	3,77	31
9	2869	812	4,21	28
10	3871	1002	4,65	26
11	5083	1212	5,09	24
12	6525	1442	5,53	22

The poisoning experiment shows that only 10 % of Hg (corresponding to 0.10 equivalent of all the ruthenium atoms) is sufficient to poison all of the available active sites of Ru(0) nanoclusters. By assuming a 1/1 *Hg/Ru(0)* stoichometry for the poisoning , one obtains 10 % of the total ruthenium atoms to be active in catalysis.

For the 2.68 ± 1.12 nm size ruthenium(0) nanoclusters, 42 % of the ruthenium atoms are on the surface. Thus, the percaentage of the active surface atoms is (10/42)×100 = 24 %. In other words, 42 % of the ruthenium atoms are on the surface and only 24 % of them are active.

5.4.6. The Catalytic Life Time Of Acetate Stabilized Ru(0) Nanoparticles (TTO's and TOF)

The rate referred to the number of catalytic cycles is known as *turnover rate,* v_t, or *turnover frequency* (TOF). It is simply defined as the number of the catalytic cycle per unit time.[62] The total turnover number of acetate stabilized-ruthenium(0) nanoclusters in the hydrolysis of sodium borohydride was found to be 4100 total turnovers over 1.4 hours (84 min) and turnover frequency of 48 min-1. These TOF and TTO values are apparent values referring to the total number of ruthenium(0) atoms in the nanoparticles. In the light of both mercury poisoning experiment and Schmid's formula, it was found that 42 % of total ruthenium(0) atoms are surface ruthenium(0) atoms in ruthenium(0) nanoclusters and only 24 % of these atoms are active. Consequently, the true maximum TOF and maximum TTO values for the Ru(0) nanoparticles are a factor of 10 higher than the apparent (lower limit) TOF of 48 min^{-1} and TTO of 4100. Therefore, the TOF increases to 480 min^{-1} and TTO's value increases to 41000 total turnovers per true active site. These values again illustrate that the use and significance of poisoning data. The TOF and TTO for both apparent and true values are given in Table 5.6.

Table 5.6. Summary of the catalytic activity of the soluble Ru(0) nanoclusters. Units of TOF values are min^{-1}.

TOF (based on total Ru atoms)	48
TOF (referred to the number of the active Ru atoms)	480
TTO's (based on total Ru atoms)	4100
TTO's (corrected for no of active Ru atoms)	41000

5.4.7. Reusability Of Acetate-Stabilized Ruthenium(0) Nanoclusters

The isolated and dried ruthenium(0) nanoparticles were tested for their catalytic activity in the hydrolysis of sodium borohydride after 2 days of storage. The catalytic activity measured for the ruthenium(0) nanoparticles after isolation, storage, and redispersing in water was compared with the catalytic activities of the original ruthenium(0) nanoparticles and ruthenium(III) chloride as given in Figure 5.18. The isolated ruthenium(0) nanoparticles could be easily dispersed in water and giving rise to a transperent dark brown colloidal solution of ruthenium. After two days of storage isolated Ru(0) nanoparticles were found to be highly active catalyst in the hydrolysis of sodium borohydride. The reaction rates were given in Table 5.7, indicate when redispersed ruthenium(0) nanoclusters retain 40 % of their catalytic activity in the hydrolysis of sodium borohydride.

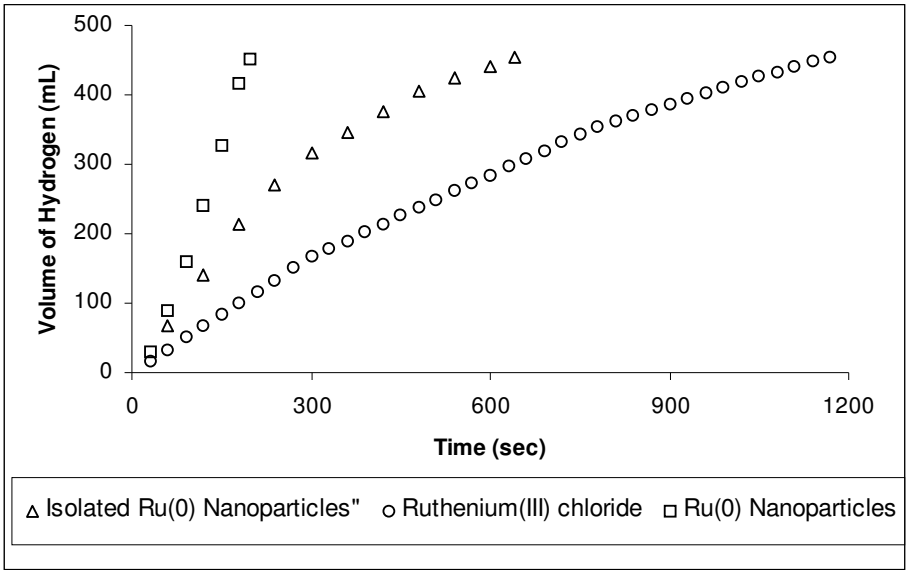

Figure 5.18. The volume of hydrogen versus time during the hydroysis of sodium borohydride.

Table 5.7. Reaction rates for the hydrolysis of sodium borohydride.

Catalyst	**($[NaBH_4]\cdot s^{-1}$)**
$RuCl_3$	0.37
Ru(0) nanoclusters	2.54
Ru(0) nanoclusters (isolated and stored 2 days)	1.01

One more outcome from the lifetime experiment is that the increasing concentration of the hydrolysis product, metaborate, doesn't have any descernable effect on the catalytic activity. During lifetime experiment the hydrogen evolution rate remains constant up to 70% conversion eventhough, the concentration of metaborate ion increases from zero at the beginning to a very high value (about 0.3 M).

CHAPTER 6

CONCLUSIONS

In summary, our study on the synthesis and characterization of Ru(0) nanoparticles as catalyst in the hydrolysis of sodium borohydride have led to the following conclusions and insights, some of which were previously unavailable:

* Using different procedures water soluble ruthenium(0) nanoclusters can be obtained from commercially available precursor material ($RuCl_3.xH_2O$) and stabilized by different ligands (acetate, ethylenediamine, dodecanethiol/acetate) in aqueous solution.

* It was found that acetate stabilized water soluble ruthenium(0) nanoclusters (2.62±1.18 nm) are highly active catalyst in the hydrolysis of sodium borohydride.

$$NaBH_4 + 2H_2O \xrightarrow{\text{Ru(0) nanoclusters}} NaBO_2 + 4H_2$$

* Sodium borohydride can be used as fuel source since it provides a safe and practical mean of producing hydrogen at normal temperature, when ruthenium(0) nanoclusters are used as catalyst.

* The rate law of the acetate stabilized, water-soluble Ru(0) nanoparticles catalyzed hydrolysis of sodium borohydride can be given as;

$$\frac{-4d[NaBH_4]}{dt} = \frac{d[H_2]}{dt} = k[Ru]$$

* Acetate stabilized ruthenium(0) nanoclusters are highly active catalyst with long lifetime providing 4100 total turnovers in the hydrolysis of sodium borohydride over 1.4 hours before they are deactivated. The recorded turnover frequency (TOF) was 48 min^{-1}. In the light of poisoning experiment the true maximum total turnover number was found to be 41000 turnovers over 1.4 hours and the true maximum turnover frequency was 480 min^{-1} per active ruthenium site.

* The activation energy (E_a = 29.2 $kJ.mol^{-1}$) of the catalytic hydrolysis of sodium borohydride using the acetate stabilized ruthenium(0) nanoclusters as catalyst is the lowest value ever found for this reaction. In alkaline solution containing 10% NaOH, the activation energy was found to be larger (E_a = 43.3 $kJ.mol^{-1}$) than this value, however, it is still smaller than the activation energy reported for the bulk ruthenium metal. Furthermore, the catalytic activity of the ruthenium nanoparticles is high even at room temperature. Therefore, these nanoparticles can be used as catalyst even at ambient temperatures in the hydrolysis of sodium borohydride.

REFERENCES

[1] Veziroğlu, T.N., **2000.** *Int. J. Hydrogen Energy.*, Proceeding of 3rd International Conference on Hydrogen Treatment Materials, **2001**.

[2] A report from the Basic Energy Sciences Advisory Committee, February, **2003.** (http://www.sc.doe.gov/bes/hydrogen.pdf)

[3] Sossina, M.H., *Acta Materialia.,* **2003**, 51, 5981-6000

[4] (a) Amendola S.C.; Onnerud, P.; Kelly, M.T.; Petillo, P.J; Sharp, G.L.; Binder, M., *J.Power Source,* **2000**, 85, 186. (b) Amendola S.C.; Janjua, J.M.; Spencer, N.C.; Kelly, M.T.; Petillo, P.J.; Sharp, G.L.; Binder, M., *Int. J. Hydrogen Energy,* **2000**, 25, 969. (c) Lee, J.Y.; Lee, H.H.; Lee, J.H.; Kim, D.M.; Kim, J.H., *J. Electrochem. Soc.,* **2002**, 149(5), 603.

[5] Zuttel, A.; Sclapbach, L., *Nature* **2001**, 414, 353.

[6] Schlesinger, H.I.; Brown, H.C.; Finholt, A.B.; Gilbreath, J.R.; Hockstra, H.R.; Hydo, E.K., *J.Am.Chem.Soc*., **1953**, 75**,** 215.

[7] (a) Levy, A.; Brown, J.B.; Lyons, C.J., *Ind. Eng. Chem.,* **1960**, 52, 211. (b) Kaufman, C.M.; Sen, B., *J. Chem. Soc. Dalton Trans.*; **1985**, 307. (c) Brown, H.C.; Brown, C.A., *J. Am.Chem.Soc*., **1962**, 84, 1493.

[8] James, B.D.; Wallbridge, M.G.H., *Prog. Inorgnic Chem.*, **1970,** 11, 99.

[9] Aicllo, R.; Sharp, J.H.; Matthews, M.A.; *Int. J. Hydrogen Energy*; **1999**, 24, 1123.

[10] Amendola, S.C.; Janjua, J.M.; Spencer, N.C; Kelly, MT.; Petillo, P.J.; Sharp, G. S.L.; Binder, M., *Int. J. Hydrogen Energy*, **2000**, 25, 969.

[11] Davis, W.D.; Mason, L.S.; Stegaman, G.; *J. Am. Chem. Soc.*, **1949**, 71, 2775.

[12] (a) Korobov, II; Mozgina, N.G.; Blinova L.N., *Kinet. Catal.*, **1995**, 48(3), 380. (b) Kim, J.H.; Lee, H.; Han, S.C.; Kim, H.S.; Song, M.S.; Lee, J.Y., *Int. J. Hydrogen Energy,* **2004**, 29, 263. (c) Hua, D.; Hanxi, Y.; Xinping, A.; Chuansain, C., *Int. J. Hydrogen Energy*, **2003**, 28, 1095. (d) Kojima, Y.; Suzuki, K.I.; Fukumoto, K.; Sasaki, M.; Yamamoto, T.; Kawai, Y.; Hayashi, H.; *Int. J. Hydrogen Energy*, **2002**, 27, 1029.

[13] (a) Roucoux, A.; Schulz, J.; Patin, H., *Chem Rev.*, **2002**, 102, 3757. (b) Widegren, J.; Finke, R.G., *Journal of Molecular Catalysis (A: Chemical)*, **2003**, 198, 317. (c) Özkar, S.; Finke, R.G.; *J. Am. Chem. Soc.*, **2002**, 124, 5796.

[14] Shriver, D.F.; Atkins, P.W., *Inorganic Chemistry*, 3rd Edition, **1999**, Oxford-University Press

[15] Klabunde, K.J.; Stark, J.; Koper, C.; Park, D., *J. Phys. Chem.,* **1996**, 100, 12142.

[16] (a) Lin, Y.; Finke, R.G., *J. Am. Chem. Soc.*, **1994**, 116, 8335. (b) Özkar, S.; Finke, R.G., *J. Am. Chem. Soc.*, **2005**, 127, 4800.

[17] Bönneman, H.; Braun, G.A., *Angew Chem. Int. Ed. Eng.*, **1996**, 35, 1992.

[18] Lewis, L.N.; Lewis, N., *J. Am. Chem. Soc.*, **1986**, 108, 7228.

[19] Schmidt, T.C.; Noeske, M.; Gasteiger, H.A.; Behm, R.J.B.; Brijoux, W.; Bönnemann, H., *Langmuir*, **1997**, 13, 2591.

[20] Vargaftik, M.N.; Zargorodnikov, V.P.; Stolarov, L.P.; Moiseev I.I.; Kochubey, D.I., *J. Mol. Cat.*, **1989**, 53, 315.

[21] Reetz, M.T.; Quaiser, S.A.; Merck, C., *Chem. Ber*., **1996**, 129, 741.

[22] Reetz, M.T.; Breinbauer, R.; Wanninger, K.; *Tet. Lett*., **1996**, 37, 4499.

[23] Reetz, M.T.; Lohmer, G., *J. Chem. Soc., Chem. Commun.*, **1996**, 39, 1921.

[24] Reetz, M.T.; Breinbauer, R.; Wedemann, P.; Binger, P.; *Tetrahedron*, **1998**, 54,1233.

[26] (a) *Clusters and Colloids; From Theory to Applications*., G.Schmid (Ed.), VCH Publishers, New York, **1994**.(b*) Physics and Chemistry of Metal Cluster Compounds.*, L.J De Jong (Ed.), Kluwer Publications **1994**.

[27] Simon, U.; Schön, G.; Schmid, G., *Angew Chem. Int. Ed. Eng*., **1990**, 248, 1186.

[28] Glanz, J., *Science*, **1995**, 269, 1363.

[29] Antonietti, M.; Göltner, C.; *Angew Chem. Int. Ed. Eng.*, **1997**, 36, 910.

[30] Elghanian, R.; Storhoff, J.J.; Mucic, R.C.; Setinger, R.L.; Mirkin, C.A.; *Science*, **1997**, 277, 1078.

[31] Colvin, V.L.; Schlamp, M.C.; Alivisatos, A.P., *Nature*, **1994**, 370, 354.

[32] Vossmeyer, T.; Delenno, E.; Heath, J.R., *Angew Chem. Int. Ed. Eng*., **1997**, 36, 1080.

[33] (a)Schmid, G.; Maihack, V.; Lantermann, F.; Pechel, S.; *J. Chem. Soc. Dalton Trans.*, **1996**, 199, 589 (b) Lin, Y.; Finke, R.G., *J. Am. Chem. Soc.*, **1994**, 116, 8335. (c) Bönneman, H.; Braun, G.A., *Angew Chem. Int. Ed. Eng*., **1996**, 35, 1992. (d) Lewis, L.N.; Lewis, N., *J. Am. Chem. Soc.*, **1986**, 108, 7228. (e) Wilcoxon, J.P.; Martinho, T.; Klavetter, E.; Sylwester, A.P., *Nanophase Mater*. **1994**, 771. (f) Na, Y.; Park, S.; Bong, S.H.; *J. Am. Chem. Soc.*, **2004**, 126, 250. (g) Pelzer, K.; Vidoni, O.; Phillot, K.; Chaudret, B.; Colliére, V., *Adv. Func. Mater*., **2003**, 12, 118. (h) Hostetler,

M.; Wingate, J.; Zong, C.; Evans, N.; Murray, R., *Langmuir*, **1998**, 14, 17-30 (ı) Pelzer, K.; Phillot, K.; Chaudret, B., *Z. Anorg. Allg. Chem*, **2003**, 629, 1217.

[34] Günter, Schmid., *Adv. Engin. Mater.*, **2001**, 3, 737

[35] (a) Finke, R.G., *In Metal Nanoparticles: Synthesis, Characterization and Applications*. Mercel-Dekker, New-York, *2002*, *Chapter 2*. (b) Blum, J.; Amer, I.; Zoran, A., *Tet. Letters,* **1983**, 24, 4139. (c) Aiken, J.D.; Lin, Y.; Finke, R.G.; *J. Mol. Catal. A: Chem.*, **1996**, 29, 114. (d) Ozkar, S.; Finke, R.G., *J. Am. Chem. Soc*. **2002**, 124, 5796-5810

[36] Evans, D.F.; Venerstöm, H., *The Colloidal Domain, 2nd Ed., Wiley, Newyork*, **1999**.

[37] Brooks, J.H.; Finke, R.G., *Chem. Mater*., **2003**, 15, 899

[38] Bönnemann, H.; Brijoux, W., *Nanostruct. Mater.*, **1995**, 5, 135.

[39] Vidoni, O.; Philippot, K.; Amiens, C.; Chaudret, B.; Balmes, O., *J. Angew Chem. Int. Ed. Eng*., **1999**, 38, 3736.

[40] Youk, J.H.; Lockin, J.; Xia, C., *Langmuir*, **2001**, 17, 4681.

[41] Zhou, Y.; Wang, J.; Zhu, Y.R.; Chen, Z.Y.; *Chem. Mater*., **1999**, 11, 2310.

[42] Klabunde, K.J.; Habdas, J., *Chem. Mater*., **1989**, 1, 481

[43] Reetz, M.T.; Helbig, W., *J. Am. Chem. Soc*., **1994**, 116, 7401.

[44] Tano, T.; Esumi, K.; Megura, K.; *J. Colloid Interface Sci.*, **1989**, 80, 84.

[45] Tano, T.; Esumi, K.; Megura, K., *J. Colloids and Surface*., **1992**, 62, 255.

[46] Bradley, J.; Millar, J.; Hill, E.; Behal, S.; Chaudret, B., *Faraday Discuss*., **1991**, 92, 255.

[47] Schmid, G.; *Endeavour New Series*., **1990**, 14, 172.

[48] Watzky, M.; Finke, R.G., *J. Am. Chem. Soc*., **1997**, 119, 10382.

[49] Schmid, G.; Morun, B.; Malm, J.*, Angew. Chem. Int. Ed. Eng*., **1989**, 28, 778.

[50] Schmid, G., *Polyhedron*, **1998**, 7, 2321.

[51] Isawa, Y., *Tailored Metal Catalysts,* Kluwer, Dordrecht, **1996**.

[52] Yang, J.; Deivaraj, T.C.; Too, H.P.; Lee, J.Y.; *Langmuir*, **2004**, 20(10), 4241.

[53] Viau, G.; Brayner, R.; Poul, L.; Chakroune, N.; Lacaze, E.; Vincent, F.; *Chem. Mater.* **2003**, 15, 486-494.

[54] Jim, Y.L.; Jun, Y.; Deivaj, T.C.; Heng-Phon, T, *J. Colloid and Interface Sci.,* **2003**, 268, 77-80

[55] Hutchison J.E.; Woehrle, G.H.; Özkar, S.; Finke, R.G., *Mater. Charact*. submitted

[56] Brooks, J.H.; Finke, R.G., *Chem. Mater*., **2004**, 16, 139.

[57] *Catalysis and Electrocatalysis at Nanoparticle Surfaces*. Edited by Andrzej Wiechowski, Marcel Dekker Inc. **2003**

[58] Broomhead, J.; Maguire, L.P.; *J. Chem. Soc*. **1967**, A4, 546.

[59] Skoog, A.D.; Holler, F.J.; Nieman, T.A., *Principles of Instrumental Analysis*, 5 th Edition, Brooks/Cole Publishing, **1997**.

[60] Levine, I.N., *Physical Chemistry 3rd edition* ; McGraw-Hill Book Company., **1998**

[61] Maxted, E. B., *Adv. Catal*., **1951**, **3**, 129.

[62] Boudart, M., *Chem. Rev.*, **1995**, **95**, 661.

APPENDIX A

The catalytic activity of $[Ru(0)]_nL_x$ (L=ethylenediamine, acetate/dodecanethiol, acetate) in the hydrolysis of sodium borohydride. $[NaBH_4]$ =150mM, $[(Ru(0))_nL_x]$=0.4mM, 25 ^oC.

	Dodecanethiol/Acetate stabilized Ru(o) Nanoparticles	***Acetate stabilized Ru(0)Nanoparticles***	***Ethylenediamine stabilized Ru(0) Nanoparticles***
Time(sec)	**Volume of Hydrogen(mL)**	**Volume of Hydrogen(mL)**	**Volume of Hydrogen(mL)**
20	32.29		
30		70.65	21.59
40	113.83		
60	168.78	153.08	60.84
80	223.73		
90		239.43	101.67
100	278.68		
120	333.63	355.51	151.11
140	372.88		
148		451.38	
150			209.99
160	425.86		
180	451.38		276.71
200			
210			343.44
220			
240			407.22
260			
270			451.38

Volume of hydrogen generated versus time for ruthenium(0) nanoparticles catalyzed hydrolysis of sodium borohydride in different Ru(0) concentrations. [$NaBH_4$]=150 mM,25 ^oC.

Time(sec)	0.1 mM	0.2mM	0.4mM	0.6mM	0.8mM	1.0mM	1.4mM
30	9.8	21.6	29.4	70.7	88.3	111.9	145.2
60	19.6	60.8	88.3	153.1	211.9	253.2	357.2
73							451.4
90	31.4	101.7	158.9	239.4	361.1		
95						451.4	
108					451.4		
120	49.1	151.1	239.4	355.5			
150	68.7	209.9	325.8				
148				451.4			
180	92.2	276.7	416.1				
198			451.4				
210	117.8	343.4					
240	139.3	407.2					
270	160.9	451.4					

The change in concentration of sodium borohydride with respect to time at constant Ru(0) concentration.

[Ru(0)]=0.4 mM. 25 ^{o}C.

Time(sec)	[$NaBH_4$](mM)	[$NaBH_4$](mM)	[$NaBH_4$](mM)
0	40	80	200
10	28.6	70.8	192.5
20	20.3	64.2	185.9
30	13.7	57.7	179.4
40	7.2	51.1	172.8
50	0.68	44.5	166.3
60		37.9	159.7
70		31.4	153.1
80		24.8	146.6
90		18.2	139.9
100		11.7	133.4
110		5.15	126.8
120		0.51	120.3
130			113.7
140			107.1
150			100.6
160			93.9
170			87.4
180			80.8
190			74.3
200			67.7
210			61.1
220			54.6
230			47.6
240			40.9
250			34.4
260			27.4
270			20.8
280			14.0
290			9.4
300			2.9

The volume of hydrogen with respect to time in Ru(0) nanoparticles catalyzed hydrolysis of sodium borohydride at constant Ru(0) and $NaBH_4$ concentrations, [Ru(0)]=0.4 mM, [$NaBH_4$]=150 mM, at different temperatures.

t	30 °C	35 °C	40 °C	45 °C
Time(sec)	Volume Of Hydrogen (mL)	Volume of Hydrogen (mL)	Volume of Hydrogen (mL)	Volume of Hydrogen (mL)
30	37.3	40.2	56.9	66.7
60	76.5	96.2	113.8	133.5
90	117.8	146.2	172.7	200.2
120	159.9	201.2	241.4	270.8
150	196.3	253.2	306.2	335.6
180	235.5	311.1	357.2	404.3
210	274.8	362.1	425.9	474.9
240	314.0	410.2	472.9	541.7
270	352.3	454.3	522.1	618.2
300	383.7	500.4	567.2	
330	445.5	541.7	618.2	
360	476.9	584.8		
390	512.2	618.2		
420	543.6			
450	572.1			
480	604.5			
500	618.2			

The volume of hydrogen with respect to time at different temperatures for Ru(0) nanoparticles catalyzed hydrolysis of sodium borohydride, [Ru(0)]=0.4 mM, [$NaBH_4$]=150mM, in alkaline solution contains 10% NaOH (w/w).

t	25 °C	35 °C	45 °C	55 °C
Time(sec)	Volume of Hydrogen (mL)	Volume of Hydrogen (mL)	Volume of Hydrogen (mL)	Volume of Hydrogen (mL)
30	9.8	19.6	29.4	43.2
60	19.6	39.3	58.9	86.4
90	29.4	59.3	88.3	133.5
120	38.4	78.6	117.7	176.6
150	48.0	97.3	147.2	
169				219.8
180	57.4	116.5	176.6	
208			219.0	
210	66.4	135.4		
240	75.6	154.3		
270	84.8	173.6		
300	93.0	192.4		
330	102.7	211.3		
349		219.3		
360	111.6			
390	120.0			
420	129.9			
450	138.9			
480	147.9			
510	156.9			
540	165.5			
570	174.4			
600	183.4			
630	192.5			
660	201.5			
690	210.9			
720	219.5			

The volume of hydrogen generated with respect to time for Ru(0) nanoparticles catalyzed hydrolysis of sodium borohydride with different concentration of stabilizing agents, [$NaBH_4$]=150mM, [Ru(0)]=0.4mM, at 25 ^oC.

[OAc^-]	0.5mM	0.8mM	1.0mM	1.5mM	2.0mM	10mM
Time	Volume of Hydrogen (mL)	Volume of Hydrogen (mL)	Volume of Hydrogen (mL)	Volume of Hydrogen (mL)	Volume of Hydrogen (mL)	Volume of Hydrogen (mL)
30,0	41,2	69,7	29,4	72,7	70,7	60,8
60,0	70,7	119,7	88,3	127,6	125,6	111,9
90,0	96,2	168,8	159,0	182,3	178,6	155,0
120,0	119,7	219,8	239,4	237,4	231,6	192,3
150,0	157,0	268,9	325,8	292,5	276,7	229,6
180,0	186,4	319,9	416,1	347,6	323,8	264,9
198,0			451,4			
210,0	206,1	369,0		402,1	367,0	302,2
234,0				451,4		
240,0	237,5	420,0			410,2	331,7
260,0		451,4				
270,0	261,0				451,4	361,1
300,0	284,6					392,5
330,0	306,2					420,0
360,0	327,4					451,4
390,0	353,3					
420,0	372,9					
450,0	394,5					
480,0	414,1					
510,0	431,8					
540,0	451,4					